การหมักสองเฟสสำหรับการผลิตกรดไอทาโคนิคโดย *Aspergillus terreus* NRRL1960 และการวิเคราะห์เอนไซม์กับทรานสคริปโตม

นางสาวปาจรียา ส่งเสริม

วิทยานิพนธ์นี้เป็นส่วนหนึ่งของการศึกษาตามหลักสูตรปริญญาวิทยาศาสตรดุษฎีบัณฑิต
สาขาวิชาเทคโนโลยีชีวภาพ
คณะวิทยาศาสตร์ จุฬาลงกรณ์มหาวิทยาลัย
ปีการศึกษา 2559

TWO-PHASE FERMENTATION FOR ITACONIC ACID PRODUCTION BY *Aspergillus terreus* NRRL1960 AND ITS ENZYMATIC AND TRANSCRIPTOMIC ANALYSES

Miss Pajareeya Songserm

A Dissertation Submitted in Partial Fulfillment of the Requirements
for the Degree of Doctor of Philosophy Program in Biotechnology
Faculty of Science
Chulalongkorn University
Academic Year 2016

Thesis Title	TWO-PHASE FERMENTATION FOR ITACONIC ACID PRODUCTION BY *Aspergillus terreus* NRRL1960 AND ITS ENZYMATIC AND TRANSCRIPTOMIC ANALYSES
By	Miss Pajareeya Songserm
Field of Study	Biotechnology
Thesis Advisor	Associate Professor Nuttha Thongchul, Ph.D.
Thesis Co-Advisor	Associate Professor Aphichart Karnchanatat, Ph.D.
	Professor Shang-Tian Yang, Ph.D.

Accepted by the Faculty of Science, Chulalongkorn University in Partial Fulfillment of the Requirements for the Doctoral Degree

.....Dean of the Faculty of Science
(Associate Professor Polkit Sangvanich, Ph.D.)

THESIS COMMITTEE

.....Chairman
(Associate Professor Nattaya Ngamrojanavanich, Ph.D.)
.....Thesis Advisor
(Associate Professor Nuttha Thongchul, Ph.D.)
.....Thesis Co-Advisor
(Associate Professor Aphichart Karnchanatat, Ph.D.)
.....Thesis Co-Advisor
(Professor Shang-Tian Yang, Ph.D.)
.....Examiner
(Assistant Professor Kittinan Komolpis, Ph.D.)
.....Examiner
(Assistant Professor Kanoktip Packdibamrung, Ph.D.)
.....External Examiner
(Associate Professor Kaemwich Jantama, Ph.D.)

ปาจรียา ส่งเสริม : การหมักสองเฟสสำหรับการผลิตกรดไอทาโคนิคโดย *Aspergillus terreus* NRRL1960และการวิเคราะห์เอนไซม์กับทรานสคริปโตม (TWO-PHASE FERMENTATION FOR ITACONIC ACID PRODUCTION BY *Aspergillus terreus* NRRL1960 AND ITS ENZYMATIC AND TRANSCRIPTOMIC ANALYSES) อ.ที่ปรึกษาวิทยานิพนธ์หลัก: รศ. ดร. ณัฏฐา ทองจุล, อ.ที่ปรึกษาวิทยานิพนธ์ร่วม: รศ. อภิชาติ กาญจนทัต, ศ. ดร. Shang-Tian Yang, 97 หน้า.

ในกระบวนการหมักกรดไอทาโคนิค โดยทั่วไปมักประสบปัญหาความเข้มข้นและอัตราผลผลิตต่ำ เนื่องจากไม่สามารถควบคุมสมดุลของฟลักซ์ของสารเมแทบอไลท์ที่เกี่ยวข้องในการผลิตได้ งานวิจัยนี้เสนอแนวทางเพื่ออธิบายกลไกการผลิตกรดไอทาโคนิคและหาสาเหตุของปัญหาดังกล่าวข้างต้น เพื่อนำมาปรับปรุงการผลิตกรดไอทาโคนิคต่อไป โดยแนวทางแรก เน้นการควบคุมการสร้างพลังงาน ATP เพื่อทดแทนในระหว่างกระบวนการผลิตกรดไอทาโคนิคโดยการเติม L-aspartate จากการทดลองพบว่าเมื่อเติม L-aspartate เข้มข้น 10 mM ลงในอาหารเลี้ยงเชื้อในระยะการหมักโดย *A. terreus* ส่งผลให้แอคติวิตี้ของไพรูเวทคาร์บอกซิเลสลดลง ซึ่งทำให้ฟลักซ์ของมาเลทในไซโทซอลลดลง ก่อให้เกิดการเคลื่อนที่ของไพรูเวทฟลักซ์กลับเข้าในไมโทคอนเดรีย ก่อให้เกิดการเพิ่มฟลักซ์ของซิส-อะโคนิเททซึ่งเป็นสารตัวกลางในการผลิตกรดไอทาโคนิคผ่านทางแอนติพอร์เทอร์ ท้ายที่สุดส่งผลให้อัตราผลผลิตต่อกลูโคสและความเข้มข้นสุดท้ายของกรดไอทาโคนิคเพิ่มขึ้นเป็น 8.33% และ 60.32% ตามลำดับ ในแนวทางที่สอง ได้ประยุกต์ใช้กระบวนการหมักแบบ 2 เฟส โดยพบว่ากรดไอทาโคนิคจะถูกสังเคราะห์ขึ้นเมื่อปริมาณแอมโมเนียมและฟอสเฟตถูกจำกัด นอกจากนี้แล้วยังพบว่า ในกระบวนการหมักแบบ 2 เฟสไม่ต้องการปริมาณออกซิเจนสูงซึ่งแตกต่างจากในกระบวนการหมักเดิมแบบ 1 เฟส ทั้งนี้พบว่า เมื่อค่าการละลายของออกซิเจนในน้ำหมักถูกควบคุมไว้ที่ระดับต่ำ จะส่งผลให้ราเจริญเติบโตอยู่ในลักษณะสัณฐานในรูปของ mycelia clump ที่เอื้อต่อการผลิตกรดไอทาโคนิค นอกจากนี้พบว่าค่าการละลายของออกซิเจนที่ต่ำยังทำให้กระบวนการสับสเตรทเลเวทฟอสฟอริเลชั่นถูกกระตุ้นเพื่อใช้ในการสร้างพลังงาน ATP ทดแทน เนื่องจากกระบวนการไกลโคไลซิสและกระบวนการออกซิเดทีฟฟอสฟอริเลชั่นไม่สามารถทำงานร่วมกันได้เมื่อปริมาณออกซิเจนมีไม่เพียงพอ ซึ่งในสภาวะดังกล่าวทำให้ไพรูเวททำปฏิกริยากับโคเอนไซม์เอโดยไพรูเวทฟอร์เมทไลเอส เกิดเป็นฟอร์เมทและอะซิทิลโคเอ ซึ่งไปกระตุ้นฟลักซ์ของเมแทบอไลท์ในวิถีเมแทบอลิซึมเพื่อสังเคราะห์เป็นกรดไอทาโคนิค

สาขาวิชา เทคโนโลยีชีวภาพ ลายมือชื่อนิสิต .....

ปีการศึกษา 2559 ลายมือชื่อ อ.ที่ปรึกษาหลัก .....

ลายมือชื่อ อ.ที่ปรึกษาร่วม .....

ลายมือชื่อ อ.ที่ปรึกษาร่วม .....

5472883423 : MAJOR BIOTECHNOLOGY
KEYWORDS: ITACONIC ACID / 2-PHASE FERMENTATION / ASPERGILLUS TERREUS / METABOLIC PATHWAY / ENZYME REGULATION

PAJAREEYA SONGSERM: TWO-PHASE FERMENTATION FOR ITACONIC ACID PRODUCTION BY *Aspergillus terreus* NRRL1960 AND ITS ENZYMATIC AND TRANSCRIPTOMIC ANALYSES. ADVISOR: ASSOC. PROF. NUTTHA THONGCHUL, Ph.D., CO-ADVISOR: ASSOC. PROF. APHICHART KARNCHANATAT, Ph.D., PROF. SHANG-TIAN YANG, Ph.D., 97 pp.

Typical itaconic acid fermentation usually suffers from low product concentration and yield due to a failure to balance the metabolic flux towards itaconic acid production. In this study, two approaches were employed to better understand the root causes mentioned above and to enhance itaconic acid production. In the first approach, ATP regeneration was manipulated during itaconic acid production by using L-aspartate. The presence of 10 mM L-aspartate in the production medium repressed the pyruvate carboxylase activity. This resulted in the limited malate flux in the cytosol and the large pool of pyruvate in the mitochondria. *A. terreus* stimulated the conversion of the large pool of cis-aconitate into itaconic acid via the antiporters. Successively, itaconic acid production yield and final concentration were improved from the control by 8.33 % and 60.32 %, respectively. In the second approach, the 2-phase fermentation process was employed. Itaconic acid was first observed when ammonium and phosphate became limited. Contrary to those claimed in 1-phase fermentation, by this technique, low DO level enhanced itaconic acid production because it promoted the correct morphology in the form of mycelial clumps. Also, low DO level initiated the uncouple glycolysis and oxidative phosphorylation, which stimulated substrate level phosphorylation for ATP regeneration. The available pyruvate was then reacted with coenzyme A by pyruvate-formate lyase, resulting in formate and acetyl CoA which induced the metabolite flux to produce itaconic acid.

Field of Study: Biotechnology Student's Signature .....

Academic Year: 2016 Advisor's Signature .....

Co-Advisor's Signature .....

Co-Advisor's Signature .....

ACKNOWLEDGEMENTS

First of all, I would like to express my special appreciation and thanks to my advisor, Assoc. Prof. Nuttha Thongchul, who have been a tremendous mentor for me. Her guidance helped me in all the time of research, writing and publishing research papers as well as writing of this thesis. Also, many thanks for giving me so many excellent opportunities during my doctoral studies.

My sincere thanks also go to my co-advisor, Assoc. Prof. Aphichart Karnchanatat for many insightful discussions and suggestions. Furthermore, my profound gratitude goes to Prof. Shang-Tian Yang who also served as my co-advisor. He provided me an opportunity to visit his laboratory in William G. Lowrie Department of Chemical and Biomolecular Engineering, the Ohio State university, USA. Thus, I consider it as a great opportunity to do my research under his guidance and to learn from his research expertise.

I also greatly thankful to Assoc. Prof. Kaemwich Jantama for his fruitful discussion on transcriptomic analysis. Besides, I would like to express my sincerely gratitude to all members of thesis committee; Assoc. Prof. Nattaya Ngamrojanavanich, Asst. Prof. Dr. Kittinan Komolpis, Assoc. Prof. Kaemwich Jantama and Asst. Prof. Dr. Kanoktip Packdibamrung for their time, insightful questions and suggestions. I would also like to extend my sincere thanks to various members of my laboratory. Thanks for their help, suggestion and moral support.

Unforgettably, I gratefully acknowledge the funding sources that made my Ph.D. work possible. I was the recipient of the Royal Jubilee Scholarship Program, Thailand Research Fund.

Finally, thanks go to mum, dad, my sister and my brother for almost unbelievable support and their unconditional love. I would like to dedicate this thesis to them.

CONTENTS

Page

Page

Page

LIST OF TABLES

LIST OF FIGURES

CHAPTER 1

INTRODUCTION

1.1 Background

The depletion of fossil fuel drives the development of bio-based chemical to replace fuel based chemicals. Itaconic acid or methylene succinic acid ($C_5H_6O_4$) is one of bio-based platform chemicals which can be derived into high value-added chemicals or materials. Itaconic acid is an unsaturated 5-carbon dicarboxylic acid, which is a naturally occurring non-toxic compound. The primary use of itaconic acid was as a co-monomer in the production of Acrylonitrile-Butadiene-Styrene and acrylate latexes for paper and architectural coating materials. Moreover, there is a chance for itaconic acid to be launched in the market for the specialty chemicals as a bioactive compound for agricultural, pharmaceutical, and medical purposes (Saha, 2017; Willke and Vorlop, 2001). Most importantly, from the US Department of Energy (DOE) report, itaconic acid has been classified as one of the top 12 chemical building blocks derived from biomass that can be used as a precursor in the production of various high-value bio-based chemicals or materials (Choi et al., 2015).

Itaconic acid was discovered by Baup in 1837 as a product of pyrolytic distillation of citric acid (Willke and Vorlop, 2001). Then, it was firstly reported as a natural metabolite of *Aspergillus itaconicus*. Later, *Aspergillus terreus* was described as the robust strain for the biosynthesis of itaconic acid (Calam et al., 1939). Because of various industrial applications, the production processes for itaconic acid have long

been developed by many researchers. In 1955, Charles Pfizer & Company started an industrial production of itaconic acid via a submerged fungal fermentation process in their production facility located in Brooklyn, NY, USA (Pfeifer et al., 1952). Nonetheless, the biosynthesis route when compared with the chemical process usually suffers from a low production efficiency. As a consequence of low supply of the bio-based itaconic acid via fermentation process, it has eventually limited the demand in various applications. Since Cargill, the largest US company producing bio-based itaconic acid, exited the business, itaconic acid has been supplied by small manufacturers in UK and China. Later, *A. terreus* has been extensively used to develop the bio-based itaconic acid production process (Willke and Vorlop, 2001).

To date, itaconic acid is commercially produced from fermentation process with a production titer of 80 g/L (Okabe et al., 2009). Transparency Market Research (2015) reported that the annual worldwide itaconic acid production was estimated to be 80,000 tons per year with an approximate price of 2 US$ per kg. Due to the wide range of its application, the production capacity is expected to increase 5.5% annually between 2016 and 2023. However, the high price of this acid is a main factor limiting its market growth and the potential for replacing fossil based counterparts. Therefore, the development of the bioprocess technology that can provide both the low production cost and the sufficiently high product quantity for replacing the fossil based counterparts is necessary for promoting its market growth. (Transparency Market Research, 2015).

It was claimed that itaconic acid was a growth-associated product, occurred via the glycolytic pathway and the early step of the oxidative route in the tricarboxylic acid (TCA) cycle. The biosynthesis of itaconic acid started with breaking down a molecule

of glucose via glycolysis in the cytosol resulting in 2 molecules of pyruvate. One molecule of pyruvate was transported into the mitochondria and subsequently being converted to acetyl CoA by the pyruvate dehydrogenase complex. Citrate synthase in the mitochondria then catalyzed the reaction of acetyl CoA and oxaloacetate, followed by citrate isomerization by aconitase. Whereas another molecule of pyruvate remaining in the cytosol was carboxylated to oxaloacetate and later converted to malate (Jaklitsch et al., 1991). Itaconic acid was synthesized by decarboxylation of cis-aconitate in the cytosol. To achieve that, cis-aconitate in the mitochondria was transported via the malate-citrate transporter while malate was transferred from the cytosol to the mitochondria to maintain the metabolic flux balance. From the proposed metabolic conversion of itaconic acid that involved several bioconversion reactions and transport of metabolites across the cell compartments, this remained process optimization to enhance itaconic acid production challenging.

Previous literatures found that ATP was required during itaconic acid fermentation, and itaconic acid production stopped when ATP formation was inhibited. It was claimed that ATP was perhaps required for maintaining a proper physiological pH (near neutral pH) inside the cells, counteracting the acid produced in the fermentation process and the low external pH (below 2.0); thus responsible for itaconic acid transport throughout the cell. This strongly indicated the need of ATP in maintaining itaconic acid fermentation.

In addition, other factors were claimed to influence itaconic acid production including high glucose concentration, nutrient limitation (manganese, ammonium, and phosphate), low pH and high oxygen supply (Klement and Buchs, 2013). The typical

itaconic acid fermentation usually experienced the low final product concentration and yield due to the failure to balance the metabolite flux towards itaconic acid production.

Therefore, the first objective of this study was to increase the availability of ATP during itaconic acid fermentation by inhibiting pyruvate carboxylase (PC). By this inhibition, more ATP would be available for itaconic acid production and transport, which eventually would result in improved yield and productivity. PC, a biotin-dependent carboxylase, converts 1 mol of pyruvate into 1 mol of oxaloacetate (OAA) with supplemented 1 mol of CO_2 and 1 mol of ATP input. The in vitro inhibition of fungal PC has been documented. Purified PC of *Rhizopus arrhizus* was inhibited by L-aspartate and 2-oxoadipate (Osmani and Scrutton, 1984). PC from *Aspergillus nidulans* has also been shown to be partially inhibited by L-aspartate (Osmani et al., 1981). In this work, L-aspartate was added into the living culture of *A. terreus* to decrease the activity of PC; thus, conserving ATP for itaconic acid production and TCA products transport. The response of the living *A. terreus* on L-aspartate present in the fermentation medium during the cultivation for itaconic acid production was reported. Also, the change in metabolic flux when L-aspartate was added into the culture broth is reported in term of the fermentation kinetics and activities of the key enzymes in the pathway.

For the secondary objective in this study, to better control the metabolic flux towards itaconic acid production in bioreactor, process optimization in 2-phase fermentation was conducted. After the growth phase, *A. terreus* was cultivated in the production medium where itaconic acid production was induced. Moreover, transcriptomic analysis was performed to investigate the expression of the key genes involved in itaconic acid synthesis during the production phase of the 2-phase

fermentation process. From the expression level of the genes of interest, the bioconversion of itaconic acid production was better understood and; thus, the results obtained in this work can be employed for process optimization to further enhance itaconic acid production.

CHAPTER 2

THEORETICAL AND LITERATURE REVIEWS

2.1 Itaconic acid

Itaconic acid, or methylene succinic acid ($C_5H_6O_4$), is an unsaturated 5-carbon dicarboxylic acid. Its structure has one carboxyl group which is conjugated to the methylene group (Figure 2.1). Therefore, it can take part in addition polymerization (Willke and Vorlop, 2001).

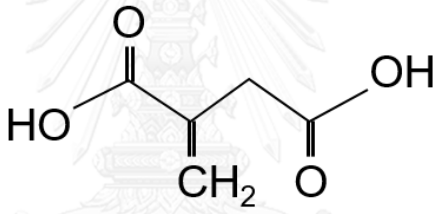

Figure 2.1 Chemical structure of itaconic acid

Itaconic acid is a naturally occurring non-toxic compound, which is readily compostable. In the solid state, it is in the form of white crystalline powder, which can dissolve in water at up to 80.1 g/L at 20°C. Itaconic acid was also found to dissolve well in alcohol including methanol, 2-propanol and ethanol (Okabe et al., 2009). The other identification and physical-chemical properties are summarized below in Table 2.1.

Table 2.1 Identification, physical and chemical properties

Parameter	
CAS number	97-65-4
EINECS number	202-599-6
H.S. code	29171960
Formula	$C_5H_6O_4$
Molecular mass	130.1 g/mol
Density	1.573 g/mL at 25°C
Boiling point	268°C
Melting point	165-168°C
Flash point	268°C
pH	2 (aqueous solution at 80mg/L)
pKa	3.85, 5.55

2.2 History of itaconic acid production

Itaconic acid was discovered by Baup in 1837 as a product of pyrolytic distillation of citric acid (Willke and Vorlop, 2001). Itaconic acid produced by a filamentous fungus was first reported by Kinoshita in 1929, and consequently this species was named *Aspergillus itaconicus*. Later, it was clarified that *Aspergillus terreus* was also responsible for the biosynthesis of itaconic acid in even higher amounts than *A. itaconicus* (Calam et al., 1939). Since that time, *A. terreus* has further been improved as the main production organism.

In 1955, Charles Pfizer & Company started the industrial production of itaconic acid via a submerged fungal fermentation process in their production facility located in Brooklyn, NY, USA (Pfeifer et al., 1952). However, the biosynthesis route, when compared with the chemical process, usually suffers from a low production efficiency

of itaconic acid. As a consequence of a low supply of the biobased itaconic acid via the fermentation process, it has eventually limited the demand in various applications. Since Cargill, a large US company that produced biobased itaconic acid, exited the business, itaconic acid has been supplied by small manufacturers in UK and China. *A. terreus* has been extensively used to develop the biobased itaconic acid production process.

Even though *A. terreus* is known currently as the primary commercial strain that produces itaconic acid, several other natural producers have been reported, (Table. 2.2) such as *Candida* sp., *Ustilago maydis*, and *Rhodotorula* sp.. Mammalian macrophages were also recently identified as itaconic acid producers (Strelko et al., 2011).

Table 2.2 Other natural producers of itaconic acid

Strain	**Itaconic acid concentration (g/L)**	**Reference**
Ustilago zeae	15	(Haskins et al., 1955)
***Candida* sp.**	35	(Tabuchi et al., 1981)
Ustilago maydis	53	(Guevarra and Tabuchi, 1990)
Psuedozyma antartica	30	(Levinson et al., 2006)
Mammalian macrophages	Not specified	(Strelko et al., 2011)

2.3 Itaconic acid application

According to its chemical structure, itaconic acid can either be self-polymerized into polyitaconic acid, or can be co-polymerized with other monomers to form heteropolymers. Thus, itaconic acid plays a crucial role as a monomer or an additive in many industrial applications, including synthetic resins, synthetic fibers, artificial glass, detergents, and paints (Willke and Vorlop, 2001). Polyitaconic acid (PIA) and styrene-butadiene rubber (SBR) latex are common end products of itaconic acid polymerization reactions. PIA can potentially replace sodium tripolyphosphate (STPP) used in detergents; while SBR latex, which is made from the polymerization of styrene, butadiene and itaconic acid, can improve water resistance in paper and card coating (El-Imam and Du, 2014).

Moreover, itaconic acid can substitute acrylic acid for use in superabsorbent polymer production with improved properties, and it can substitute maleic anhydride used in Unsaturated Polyester Resins (UPR) production. For other applications, itaconic acid can improve the adhesion of the paint in the manufacture of emulsion paints. The supplement of 5% Itaconic acid in acrylic resins can improve the resin's ability to hold printing inks. In plastics and coatings, the addition of 1-5% itaconic acid is able to improve product properties such as light colour, ease of painting and separation, water-fastness and antiseptic properties. In the medical/pharmaceutical industry, itaconic acid is used in glass ionomer cement (GIC) preparation which is very useful in restorative dentistry. In a biorefinery, itaconic acid has recently been used as a platform chemical and a precursor for several potential biofuels such as MTHF (3-MTHF) (Choi et al., 2015; Saha, 2017).

2.4 Itaconic acid biosynthesis

Since Kinoshita discovered the itaconic acid production via *A. itaconicus* and they suggested that a decarboxylation of aconitate as key reaction, the metabolic pathway for itaconic acid biosynthesis was debated for several years. Three different pathways from pyruvate to itaconic acid have been discussed, including its formation by a decarboxylation of cis-aconitate, by the condensation of pyruvate and acetyl-CoA to citramalate, or by a dehydrogenation reaction of 1,2,3-tricarboxypropanoate to aconitate and subsequently itaconic acid (El-Imam and Du, 2014).

In 1957, Bentley and Thiessen proposed the biosynthesis of itaconic acid produced via the decarboxylation of *cis*-aconitate catalyzed by the enzyme *cis*-aconitate decarboxylase (CAD). Later, this proposed pathway was confirmed by tracer

experiments using ^{14}C- and ^{13}C-labeled substrates. Also, the necessary enzymatic activities were found (Bentley and Thiessen, 1957). In 1991, Jaklitsch and co-worker discovered that the key enzyme of the pathway, CAD, isn't located in the mitochondria but in the cytosol, while the citrate synthase and aconitase are found in the mitochondria. Residual levels of aconitase and citrate synthase activity are found in the cytosolic fraction. Therefore, they proposed that cis-aconitate is transported to cytosol via the malate-citrate antiporter (Jaklitsch et al., 1991).

The above studies came to the conclusion that the pathway via aconitase and CAD was most likely the actual one (Fig.2.2). The pathway starting from one molecule of glucose, a carbon source for itaconic acid production was broken down through glycolysis into two molecules of pyruvate in the cytosol. One pyruvate molecule is transported to mitochondria and decarboxylated as well as further converted to acetyl-CoA, while the other is carboxylated to oxaloacetate and transformed into malate in the cytosol. The malate was then transported into mitochondria and consequently was converted to OAA and subsequently reacted with acetyl CoA to form citrate isomer and then cis-aconitate that was then transported into the cytosol via antiporters. Finally, it was carboxylated into itaconic acid by CAD.

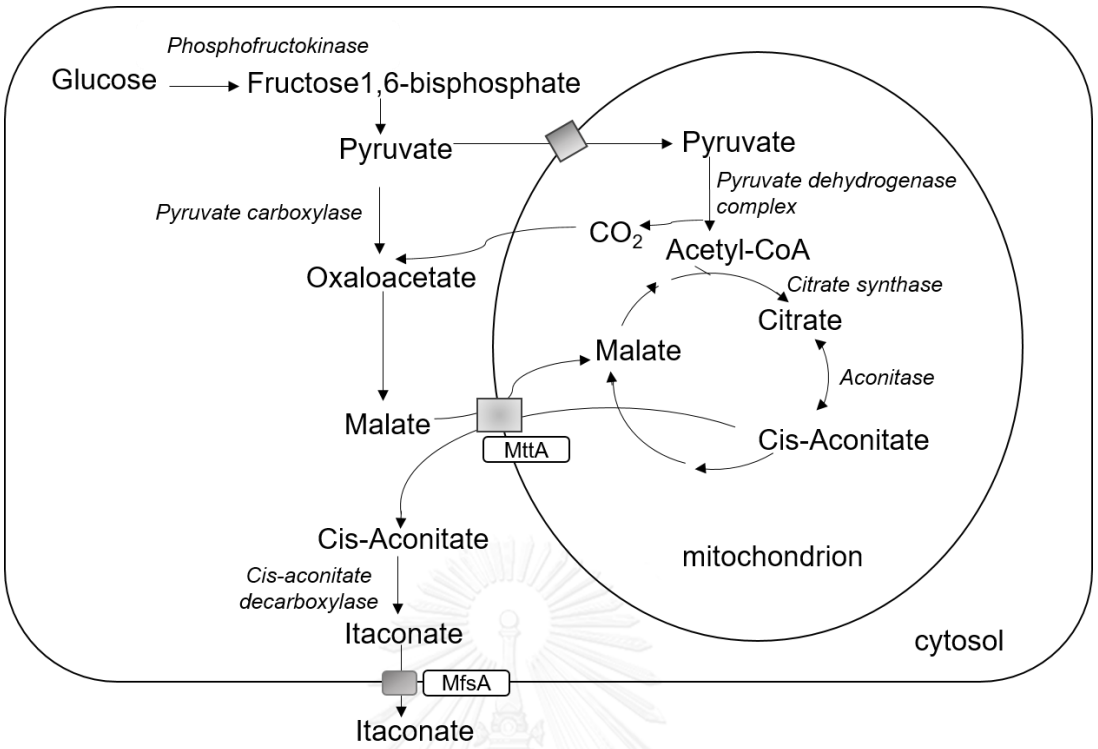

Figure 2.2 Itaconic acid pathway in *Aspergillus terreus*

2.5 *Aspergillus terreus*

The filamentous fungi *Aspergillus terreus* is classified in the Kingdom of Fungi, Division of Ascomycota, Class of Eurotiomycetes. Order of Eurotiales and Family of Trichocomaceae. *Aspergillus terreus* is a common soil saprophyte. Colonies on Czapek agar are brownish in colour and get darker as they age. It produces two types of asexual conidia, including accessory conidia (AC) which asexual conidia formed directly on hyphae and phialidic conidia (PC), in which asexual conidia arising from conidiophores generated on hyphae (Deak et al., 2009). This fungus can produce several metabolites such as geodin, itaconic acid, lovastatin, questrin, citrinin and aspulvinone (Schimmel, 1998).

2.6 Environmental factors in itaconic acid fermentation

According to the relevant literature, an interaction of several factors is needed to produce itaconic acid by *A. terreus*. It was claimed that a high glucose substrate concentration, phosphate and nitrogen limitations, high oxygen supply, low pH, and some trace elements are the essential parameters for itaconic acid production (Klement and Buchs, 2013).

2.6.1 High glucose substrate concentration

It was reported that glucose concentrations between 100 and 150 g/L were optimal for the IA fermentation process (Willke and Vorlop, 2001). Kuenz et al. (2012) found that using 120 g/L glucose achieved a final IA concentration of 65 g/L after 10 days and the substrate was consumed completely (Kuenz et al., 2012). It was suggested that high concentrations of appropriate carbon sources could repress α-keto-glutarate dehydrogenase, hence explaining the effect of the sugar concentration in terms of enzyme repression (Hossain et al., 1984).

2.6.2 Phosphate and nitrogen limitations

It was claimed that phosphate limitation and nitrogen limitation were identified as potentially growth limiting (Boer et al., 2010). When phosphate is limited, the oxidative respiration is uncoupled, resulting in decreased ATP levels and energy charge of the cell, thus, the flow through glycolysis is enhanced. Since glycolysis and respiration are uncoupled, a high metabolic flux of glucose through glycolysis into cis-aconitate and finally itaconic acid (Klement and Buchs, 2013). Moreover, a high carbon nitrogen ratio of glucose and ammonium can enhance flux through glycolysis since

ammonium may prevent the inhibition of PFK by high energy levels (Papagianni et al., 2005).

2.6.3 High oxygen supply

A strict aerobic process is one key parameter in itaconic acid fermentation (Klement and Buchs, 2013). However, there is always a conflict between the sufficient oxygen supply and the fungal cell damage by shear stress from aeration and agitation. The high itaconic acid titer needs to be closely controlled as small and frayed mycelial pellets (Gyamerah, 1995). Therefore, achieving high production usually suffer from the high oxygen supply. In literature, the optimum aeration rates for itaconic acid production were inconsistent. Thus, the appropriate aeration for specific fermentation systems needs to be determined in order to avoid either sheer stress or poor oxygen transfer rates (El-Imam and Du, 2014).

2.6.4 Low pH

A pH value less than 2 or above 5 has a negative effect on cell morphology (Klement and Buchs, 2013). Riascaldati et al. (2000) reported that the pH during itaconic acid production was the main factor which can affect the contribution of non-growth associated production. When the pH was left free to decrease from 3.4, the mycelium was severely stressed and stopped producing itaconic acid at pH 1.85 (Riscaldati et al., 2000). Moreover, it was suggested that pH could affect the concentration of each dissociation form of itaconic acid, so it had an effect on product transportation and proton-pumping (Krull et al., 2017)

2.6.5 Trace elements

Iron, calcium, copper and zinc are important co-factors for itaconic acid production (Gyamerah, 1995; Klement and Buchs, 2013). Iron is a metal ion that keeps the aconitase functional. Moreover, calcium was reported as a co-factor of several key enzymes and it had an influence on fungal morphology. In 2014, Hevekerl and co-worker found that the morphology of the pellets changed from fluffy with single hyphae to very dense form without single hyphae when without $CaCl_2$ in the medium (Hevekerl et al., 2014b).

The summary of previous studies of itaconic acid fermentation process is show in Table 2.3

Table 2.3 Summary of the previous studies of itaconic acid fermentation process

Culture method	Substrate	Culture condition	Final IA (g/L)	Production rate (g/L·h)	Yield (%)	Operation time (d)	References
Batch; Flask	Glucose	pH 2.0, 170 rpm	51.0	0.31	44	7	(Park et al., 1994)
Batch; Flask	Glucose	pH 2.0, 220 rpm	82.0	0.57	54	6	(Yahiro et al., 1995)
Batch; Stirred tank	Glucose	0.7 L/min air	30.0	0.32	55	4	(Kautola et al., 1985)
Batch; Stirred tank	Glucose	0.5 vvm, 94.2 cm/s	49.4	0.31	43	7	(Park et al., 1994)
Batch; Air lift	Glucose	pH 2.0, 0.5 vvm, 300 rpm	44.0	0.26	45	7	(Okabe et al., 2009)
Batch; Air lift	Corn starch	2 vvm	58.0	-	-	6	(Yahiro et al., 1997)
Batch; Stirred tank	Glucose	pH 2.8, 400 rpm	-	0.41	54	-	(Riscaldati et al., 2000)
Batch; Stirred tank	Sago starch	295 rpm; 0.5 vvm	48.2	-	34	5	(Dwiarti et al., 2007)
Batch; Stirred tank	Glucose	350 rpm	86.2	0.51	62	7	(Kuenz et al., 2012)
Batch; Stirred tank	Glucose	25 % DO, 470 rpm	129	1.15	58	4.7	(Hevekerl et al., 2014a)

2.7 Enzymes and genes related to the itaconic acid pathway

2.7.1 Phosphofructokinase

6-phosphofructo-1-kinase (PFK1; EC 2.7.1.11) is an enzyme that catalyzes the phosphorylation of fructose-6-phosphate (F6P) from Mg-ATP to fructose-1,6-bisphosphate and Mg-ADP. This enzyme is normally a key regulating enzyme in glycolysis. In *Aspergillus niger*, it was suggested that the enzyme could be activated by effectors like AMP, NH_4^+, Mg^{2+}, Mn^{2+} and fructose-2,6-bisphosphate, while inhibited by inhibitors like ATP and citrate (Habison et al., 1983). The shorter PFK1 fragment exhibits changed kinetics, such as resistance to citrate inhibition. An active shorter PFK1 fragment, resistant to citrate inhibition and activated to a higher level by fructose-2,6-bisphosphate with respect to the native enzyme was encoded directly from the modified gene. Capuder et al. (2009) synthesized the mutated-truncated of the *A. niger pfkA* gene encoding for the active shorter PFK1 fragment. The transformants integrated with the truncated gene accumulated up to 70% more citric acid in the same time period than the parental strain as it resisted citrate inhibition and was activated to a higher level by fructose-2,6-bisphosphate (Capuder et al., 2009). A gene was also shown effect to itaconic acid production in *A. terreus*. This truncated version of *A. niger pfkA* gene also had a positive effect on the itaconic acid production when expressed in *A. terreus* (Tevz et al., 2010).

2.7.2 Pyruvate carboxylase

Pyruvate carboxylase (PC), a biotin-dependent carboxylase that converts pyruvate into oxaloacetate (OAA) with supplemented CO_2 and one mole of ATP input. Most PCs have an α4 quaternary structure with the four identical subunits containing a biotin carboxylase (BC) domain, a carboxyl transferase (CT) domain, and a biotin carboxyl carrier protein (BCCP) domain. PC is commonly activated by the allosteric activator, acetyl CoA. Acetyl CoA stimulates ATP-cleavage and biotin reactions that occur in the active site of the BC domain. Furthermore, acetyl CoA can enhance the binding of substrates with the enzyme and also the cofactor Mg^{2+} (Adina-Zada et al., 2012). However, the inhibition of fungal PC has been documented. Purified PC of *Rhizopus arrhizus* was inhibited by L-aspartate and 2-oxoadipate (Osmani et al., 1985). PC from *Aspergillus nidulans* has also been shown to be partially inhibited by L-aspartate (Osmani et al, 1981). Moreover, it was found that avidin acted as a PC inhibitor in the bacterium *Rhizobium etli* and in the human liver, suggesting that PC avidin, which has an extremely high affinity for biotin, it is also a potent inhibitor for PC (Zeczycki et al., 2010).

2.7.3 Pyruvate dehydrogenase complex

Pyruvate dehydrogenase complex (PDC) is a multi-enzyme complex that uses three enzymatic subunits: pyruvate dehydrogenase (E1), dihydrolipoamide transacetylase (E2), and dihydrolipoamide dehydrogenase (E3), as well as an E3 binding protein (BP) (Patel et al., 2012). The oxidation of pyruvate occurs in the mitochondria of the cell where pyruvate is oxidized into acetyl-coA. In *A. terreus*, it was clarified that pyruvate dehydrogenase is exclusively localized in the mitochondrion

and involved in itaconate formation (Jaklitsch et al., 1991). PDC catalyzes the rate-limiting step in the aerobic glucose oxidation, linking glycolysis to the tricarboxylic acid cycle. The oxidative decarboxylation of pyruvate to acetyl-CoA commits the carbon atoms of glucose to two principal routes: oxidation to CO_2 by TCA cycle coupling with generation of energy, or incorporation into lipid (Berg et al., 2002). The pyruvate dehydrogenase complex is stringently controlled by several factors. High concentrations of acetyl-CoA, NADH and ATP inhibit the enzyme activity. Thus, pyruvate dehydrogenase is inactivated when the energy charge is high and biosynthetic intermediates are abundant, whereas, pyruvate as well as ADP, a signal of low energy charge, can activate the dehydrogenase. (Berg et al., 2002; Holness and Sugden, 2003).

2.7.4 Citrate synthase

Citrate synthase (CS; EC 4.1.3.7) catalyzes the reversible condensation reaction between oxaloacetate and acetylCoA yielding citrate. This reaction is the first step of the TCA cycle and functions as a rate-limiting enzyme of the cycle. The reaction starts with oxaloacetate binding to the enzyme and acetyl-CoA binding subsequently (Papagianni, 2007). However, it was reported that up to 11-fold overproduction of citrate synthase could not increase citric acid production rate in *A. niger*, suggesting that citrate synthase had a slight effect on flux control in the citric acid biosynthesis pathway (Ruijter et al., 2000). In vitro, both ATP and coenzyme A inhibit the enzyme, but it has no or a slight inhibition effect in vivo (Papagianni, 2007).

2.7.5 Aconitase

Aconitase (ACO; EC4.2.1.3), the second enzyme of the citric acid cycle, catalyzes the stereo-specific isomerization of citrate to isocitrate via cis-aconitate. In *A. niger*, it was suggested that the disappearance of aconitase is the key parameter causing citric acid to accumulate (Kubicek and Rohr, 1985). In *A. terreus*, aconitase is found in the mitochondria but a residual level of aconitase activity is also found in the cytosolic fraction (Jaklitsch et al., 1991). However, overexpression of the *acoA* that encodes this enzyme did not improve itaconic acid production levels (Huang et al., 2014).

2.7.6 Cis-aconitate decarboxylase

Cis-aconitate decarboxylase (CAD; EC 4.1.16) is a key enzyme in itaconic acid production that converts cis-aconitate to itaconic acid. In 1957, Bentley and Thiessen suggested that cis-aconitate could be a substrate of an *A. terreus* crude enzyme preparation to form itaconic acid (Bentley and Thiessen, 1957). Later it was confirmed by Bonnarme and coworkers in 1995, as they traced ^{14}C-labeled metabolites and concluded that CAD catalyzed the carboxylation of cis-aconitate to itaconic acid in the cytoplasm (Bonnarme et al., 1995). A 55-kDa protein which had CAD activity was purified from the high IA-producing strain *A. terreus* TN484-M1 (Dwiarti et al., 2002).

In 2008, Kanamasa et al. determined the N-terminal, and four internal sequences, which produced a single hit, ATEG_09971, in the genome database of *A. terreus*. The gene and its protein product was named *cadA* and CadA, respectively. Moreover, they clarified the role of CAD in the high-producing strain TN484-M1. The results showed no differences in the nucleotide sequences of *cadA* from the wild type

and TN484-M1 strains, but the *cadA* transcription level of the TN484-M1 strain was fivefold higher than that of the wild-type strain (Kanamasa et al., 2008).

Li et al. (2011) also have shown that genes involved in the biosynthesis pathway. They used a transcriptomic approach to identify the *cadA* gene. The above studies indicate that *cadA* is the key gene in the itaconic acid fermentation pathway, however nothing is known so far about the regulatory mechanisms leading to the expression of this gene (Li et al., 2011).

CHAPTER 3

EXPERIMENTAL

3.1 Apparatus and Chemicals

3.1.1 Apparatus

Apparatus	**Model**	**Manufacturer and country**
Autoclave	KT-40L	ALP Co., Ltd., Japan
Centrifuge	MC-15A	Tomy Seiko Co., Ltd., Japan
Electronic balance	ML204/01 Metter	Toledo AG, Switzerland
HPLC	Shimadzu LC 10A	Shimadzu Co., Ltd., Japan
Laminar flow hood	NK system clean bench	International Scientific Supply, Thailand
Oven	UL-80	Memmert Co., Ltd., Germany
pH meter	AB15	Fisher Scientific, Ltd., Singapore
Rotary incubator shaker	G25	New Brunswick Scientific Co., Inc., USA
Vortex mixer	K-550-GE	Scientific Industries, Inc., USA
Fermentor (5 Liter)	BIOSTAT® Bplus	Sartorius, Germany
Spectrophotometer	Multiskan Go	Thermo scientific, USA

3.1.2 Chemicals

Chemicals	**Manufacturer and country**
Acetyl CoA	Sigma, Germany
Agar	Patanasin Enterprise, Thailand
Alcohol dehydrogenase	Sigma, Germany
Ammonium chloride (NH_4Cl)	Riedel-de Haen, Germany
Ammonium sulfate $(NH_4)_2SO_4$	Merck, Germany
Bovine serum albumin (BSA)	Sigma, Germany
Calcium chloride dihydrate ($CaCl_2.2H_2O$)	Fluka, France
Citrate synthase	Sigma, Germany
Copper sulfate pentahydrate ($CuSO_4.5H_2O$)	Fluka, France
5-dithio-2-nitrobenzoate (DTNB)	Sigma, Germany
Ethanol (C_2H_5OH)	Merck, Germany
Folin phenol reagent	Sigma, Germany
Glucose ($C_6H_{12}O_6$)	Siamchai Chemical, Thailand
Hydrochloric acid (HCl)	Merck, Germany
Iron sulfate heptahydrate ($FeSO_4.7H_2O$)	Merk, Germany
Magnesium sulfate heptahydrate ($MgSO_4.7H_2O$)	Riedel-de Haen, Germany
Manganese chloride tetrahydrate ($MnCl_2.4H_2O$)	Riedel-de Haen, Germany
Nicotinamide adenine dinucleotide (NADH)	Sigma, Germany
Oxaloacetic acid	Sigma, Germany
Phosphofructokinase (PFK) Activity-Colorimetric Assay Kit	Sigma, Germany

Chemicals	**Manufacturer and country**
Potassium dihydrogen phosphate (KH_2PO_4)	Riedel-de Haen, Germany
Di potassium phosphate dibasic (K_2HPO_4)	Riedel-de Haen, Germany
Pyruvic acid	Merk, Germany
Sodium carbonate (Na_2CO_3)	Sigma, Germany
Sodium chloride (NaCl)	Sigma, Germany
Sodium hydroxide (NaOH)	Grand Chemical, Thailand
Sulfuric acid (H_2SO_4)	Sigma, Germany
Thiamine pyrophosphate (TPP)	Sigma, Germany
Yeast extract	Springer, France
Zinc Sulfate Heptahydrate ($ZnSO_4.7H_2O$)	Riedel-de Haen, Germany

3.2 Microorganism and inoculum preparation

3.2.1 Microorganism

Aspergillus terreus NRRL1960 was kindly provided by Agricultural Research Service Culture Collection, US Department of Agriculture, Peoria, IL, USA. The culture was maintained on Czapek's agar plate and subcultured every month to maintain the fungal activity.

3.2.2 Inoculum preparation

Conidiospores were harvested from the 7-day culture incubated at 30 °C by shaving and extracting the spores with the sterile deionized water. The spore concentration was adjusted to 10^6 spores/mL by diluting with the sterile deionized water. Ten millimeters of the spore suspension were used to inoculate the bioreactor.

3.3 Medium composition

3.3.1 Growth medium (per liter)

Glucose	30	g
Yeast extract	5	g

The pH of the production medium was adjusted to 3.

3.3.2 Production medium (per liter)

Glucose	100	g
$(NH_4)_2SO_4$	2.36	g
KH_2PO_4	0.11	g
$MgSO_4.7H_2O$	2.08	g
$CaCl_2.2H_2O$	0.13	g
NaCl	0.074	g
$CuSO_4.5H_2O$	0.2	mg
$FeSO_4.7H_2O$	5.5	mg
$MnCl_2.4H_2O$	0.7	mg
$ZnSO_4.7H_2O$	1.3	mg

The pH of the production medium was adjusted to 2.

3.4 Methodology

3.4.1. Improving itaconic acid production by regulating pyruvate carboxylase in the living culture of *Aspergillus terreus* NRRL 1960 by using L-Aspartate

The expression of key enzymes in the metabolic pathway and end metabolite production were determined and compared with those obtained from the culture without L-aspartate (control).

3.4.1.1 Glucose-based fermentation without L-aspartate of *A. terreus* NRRL1960 in flask fermentation (Control)

Itaconic acid fermentation by *A. terreus* consisted of 2 phases. During the growth phase, the growth medium was used to promote spore germination and initial cell growth. Then, 0.5 mL spore suspension (10^6 spores/mL) was inoculated into a 250-mL Erlenmeyer flask containing 50 mL sterile growth medium. The initial pH during growth phase was 3. The culture was incubated at 30 °C in a rotary shaker at 150 rpm for 48 h. At the end of the growth phase, the growth medium was replaced by the production medium. The pH of the production medium was initially adjusted to 2. The culture was incubated at the same conditions as those during the growth phase for another 192 h. During the fermentation, samples were taken every 12 h for analyses of cell biomass, glucose, itaconic acid, and other byproducts (see in 3.4.3) as well as for enzymatic activities (see in 3.4.1.2).

3.4.1.2 Glucose-based fermentation with L-aspartate of *A. terreus* NRRL1960 in flask fermentation

3.4.1.2.1 Effect of L-Aspartate on metabolism of *A. terreus* during growth phase

L-aspartate was added into the growth medium at different concentrations and was conducted in the similar manner to those mentioned in 3.4.1.1. During the fermentation, samples were taken every 12 h for analyses of cell biomass, glucose, itaconic acid, and other byproducts (see in 3.4.3) as well as for enzymatic activities (see in 3.4.1.2). The effects of L-aspartate on growth were investigated during the growth phases.

3.4.1.2.2 Effect of L-Aspartate on metabolism of *A. terreus* during production phase

A. terreus was pre-grown in the growth medium without L-aspartate. Then, L-aspartate was added into the production medium at different concentrations and was conducted in the similar manner to those mentioned in 3.4.1.1. During the fermentation, samples were taken every 12 h for analyses of cell biomass, glucose, itaconic acid, and other byproducts (see in 3.4.3) as well as for enzymatic activities (see in 3.4.1.2). The effects of L-aspartate on metabolite production were investigated during the production phases.

3.4.1.3 Cell extraction, partial enzyme purification and protein determination

3.4.1.2.1 Cell extraction and partial enzyme purification

Following the method described in Thitiprasert et al. (2014), fresh fungal mycelia from the fermentation were washed thoroughly with sterile DI water three times before drying between filter paper (Thitiprasert et al., 2014). Filter-dry mycelia were weighed into 1 g and frozen at −20 °C for 1 h before grinding in an ice-cold mortar for 5 min. Tris-HCl buffer (1.5 mL, 0.2 M, pH 8.0) was added into the ground mycelia. The suspension of the fungal mycelia with the glass beads was then homogenized in the cell disrupter for 16.75 min (30-s interval with45-sbreak). Later, the glass beads were removed by filtration and the suspension was then centrifuged at 12,000g for 30 min at 4 °C. The supernatant to be called later the cell extract was used for protein determination and enzyme assays.

3.4.1.2.2 Protein determination

The protein content was determined by Lowry's method using a bovine serum albumin (BSA) as a standard. Protein content was determined by the modified Lowry's method using a bovine serum albumin (BSA) as a standard. Two reagents were used in the assay, i.e. reagent A which contains 4 mL 2.0% sodium potassium tartrate, 4 mL 1% $CuSO_4.5H_2O$, and 392 mL 2.0% Na_2CO_3 in 0.1 N NaOH and reagent B that is a Folin phenol reagent. Both reagents were freshly prepared before use (Lowry et al., 1951).

BSA standard curve was prepared by diluting 2 mg/mL BSA standard with 10-100 µL distilled water (0-200 µg/mL). Then 3 mL reagent A were added. The mixture

was mixed thoroughly before incubation for 10 min. After that 0.3 mL reagent B were added into the mixture. The mixture was mixed well and incubated for another 30 min. After that the optical density of the mixture was observed at the wavelength of 650 nm.

The protein content in the cell extract sample was determined by the same method used in standard curve preparation. Three mL reagent A was mixed with 0.1 mL cell extract. The mixture was incubated for 10 min. After incubation, 0.3 mL reagent B was added into the mixture. After mixing thoroughly, the mixture was incubated for 30 min. The optical density of the mixture was measured at the wavelength of 650 nm and the protein concentration in the sample was calculated from the BSA standard curve.

3.4.1.3 Enzyme assays

3.4.1.3.1 6-phosphofructo-1-kinase (PFK)

6-phosphofructo-1-kinase (PFK) activity was determined by phosphofructokinase colorimetric assay kit (Sigma). The enzyme activity was determined from a couple enzyme reaction, in which PFK catalyzed the conversion of fructose-6-phosphate and ATP to fructose-1,6-diphosphate and ADP. ADP was later converted by the enzyme in the mixture into AMP. The reaction mixture containing 42 µL PFK assay buffer, 2 µL PFK enzyme mix, 2 µL PFK developer, 2 µL ATP, and 2 µL PFK substrate was added into a 96-well plate. Then, 10 µL crude enzyme extract was added into each well. The resulting NADH reduced the colorless indicator resulting in a colorimetric product at 450 nm proportionally to the PFK activity presenting in the enzyme mixture. The absorbance at 450 nm of the reaction mixture was recorded every 57 s for 5 min. The average rate of the increasing absorbance at 450 nm per min was

calculated. The activity of PFK was subsequently determined using the calibration plot of absorbance at 450 nm versus NADH concentration in micromoles. One unit of PFK was determined by the amount of enzyme that generated 1.0 μmol NADH per 1 min at 37°C, pH 7.4.

3.4.1.3.2 Pyruvate carboxylase (PC)

Pyruvate carboxylase (PC) was determined from a couple enzyme reaction. PC catalyzed the carboxylation of pyruvate into oxaloacetate (OAA) (Eq. 1). OAA was then reacted with acetyl CoA to form citryl-CoA by citrate synthase, which was subsequently hydrolyzed to citrate and CoA (Eq. 2). In the spectrophotometer, the rate-limiting reaction catalyzed by PC (Eq.1) is coupled to the effectively irreversible chemical reaction(Eq.3). The reaction product thionitrobenzoic acid (TNB) was the absorbing substance with intense absorption at 412 nm.

$$ATP + pyruvate + HCO^{3-} = ADP + phosphate + oxaloacetate \quad (1)$$

$$Acetyl\text{-}CoA + oxalacetate + H_2O = citrate + CoA\text{-}SH \quad (2)$$

$$CoA\text{-}SH + DTNB = TNB + CoA\text{-}S\text{-}S\text{-}TNB \quad (3)$$

PC activity was determined in the reaction mixture containing 0.050 M $NaHCO_3$, 0.005 M $MgCl_2$, 0.050 mM acetyl CoA, 0.005 M pyruvate, 0.005 M ATP, 0.200 mM 5,5'-dithio-bis(2-nitrobenzoic acid), and 5 U/mL citrate synthase in 0.1 M Tris HCl buffer (pH 8.0) in a total volume of 1.0 mL. The reaction was initiated by adding 50 μL crude enzyme extract into the reaction mixture with a run-time of 60s at the temperature of 30°C. The increase in absorbency at 412 nm of 5-dithio-2-nitrobenzoate (DTNB) was measured (Zhang et al., 2012). The PC activity was determined by using the standard curve of absorbency at 412 nm versus oxaloacetate

concentration in µmol which could react with acetyl CoA via citrate synthase, then hydrolyzed to citrate and CoA that actually causes the signal by the free CoA reaction with DTNB. One unit of PC activity was corresponded to the formation of 1 µmol oxaloacetate per 1 min at 30 °C.

3.4.1.3.3 Pyruvate dehydrogenase complex (PDC)

Pyruvate dehydrogenase complex (PDC) activity was assayed by following the depletion of NADH at 340 nm (Acar et al., 2007). The reaction mixture contained 25 mM sodium pyruvate, 5 mM $MgCl_2$, 0.2 mM thiamine pyrophosphate (TPP), 11 U/mL alcohol dehydrogenase, and 0.15 mM NADH in 100 mM MES buffer (pH 6.5) in a total volume of 1.2 mL. The reaction was started by adding diluted enzyme sample in crude extract and the absorbency at 340 nm was recorded every 57 s for 5 min at 30 °C. The average rate of the increase in absorbency at 340 nm per min was determined. PDC activity was monitored at 340 nm corresponding to the amount of NADH (in micromoles) oxidized per minute using the calibration plot of absorbency at 340 nm versus NADH concentration (micromoles).

3.4.1.3.4 Cis-aconitate decarboxylase (CAD)

Cis-aconitate decarboxylase (CAD) activity was assayed by Bently method (Kanamasa et al., 2008). Crude enzyme extract (0.1 mL) was incubated with 0.4 mL cis-aconitic acid solution (to the final concentration of 8.0 mM) and 2.5 mL sodium phosphate (0.2 M, pH 6.2) for 10 min at 37 °C. The reaction was terminated by adding 0.1 mL HCl (12.0 M). The released itaconic acid was analyzed by HPLC using the similar method described earlier.

3.4.1.3.5 Citrate synthase (CS)

Citrate synthase (CS) was assayed by DTNB method. The reaction mixture contained 0.1 M Tris HCl buffer (pH 8.0), 0.2 mM 5,5′-dithio-bis (2-nitrobenzoic acid), 0.05 mM oxaloacetate, and 0.05 mM acetyl CoA in a total volume of 1.0 mL. The reaction was started by adding 50 μL crude enzyme extract into the reaction mixture. The absorbance at 340 nm was measured every 57 s for 5 min at 30 °C; then, the average rate of the increase in absorbency at 450 nm per min was calculated. One unit of CS was defined as 1 μmol oxaloacetate converted per minute. The amount of oxaloacetate present in the reaction mixture determines from the calibration the curve of absorbency at 412 nm versus amount of oxaloacetate (in micromoles) (see in Eqs. 2 and 3).

3.4.2 Process optimization in 2-phase fermentation in the stirred-tank bioreactor for itaconic acid production by *Aspergillus terreus* NRRL1960.

The effects of C/N ratio, oxygen and pH was determined. Then, gene expression of the key enzymes responsible for itaconate production under the optimized was analyzed.

Itaconic acid production by *Aspergillus terreus* NRRL1960 was conducted in the 5-L stirred-tank bioreactor. Before operation, the bioreactor filled up with the growth medium (3 L) was autoclaved at 121 °C, 15 min for 30 min. After sterilization, the bioreactor was cool down before starting the control system. Dissolved oxygen (DO) sensor (InPro6820, Mettler Toledo) was calibrated by the pure nitrogen and air. The dissolved CO_2 sensor (InPro®5000(i) CO_2 sensor, Mettler Toledo) was calibrated with CO_2 gas before cultivation. The growth phase started by inoculating the spore

suspension (10 mL) into the bioreactor. The bioreactor was operated at 30 °C, 100 rpm, 0.5 vvm for 48 h. At the end of the growth phase, the growth medium was replaced by the sterile production medium (3 L). The culture was incubated at the same temperature with varied pH, DO levels, and the weight ratio of carbon to nitrogen sources (C/N ratio). During the fermentation, the pH was automatically controlled at the set point by 5 M KOH. The DO profile as well as the CO_2 concentration were observed during the production phase.

3.4.2.1 Determine the optimized C/N ratio of the production medium in 2-phase fermentation

To optimize the C/N ratio of the production medium, glucose/$(NH_4)_2SO_4$ ratio of 100/2.36, 100/1.68, 100/0.84 100/0.42, and 100/0.21 were initially added into the production media. The fermentation was conducted in the similar manner to those mentioned in 3.4.2. Samples was taken every 12 h until the end of the fermentation then was used to determine the fermentation kinetics (yield and productivity) as well as residual phosphate and ammoniacal nitrogen (see in 3.4.3.3 and 3.4.3.4, respectively).

3.4.2.2 Determine the optimized DO levels and pH of the production medium in 2-phase fermentation

To study the effect of pH and DO on itaconic acid production in the stirred-tank bioreactor, pH during production was controlled at different values of 1.85, 2.00, 2.15, and 2.30 by adding 5 M KOH. The percentage of DO was controlled at different concentrations of 10, 15, 20, and 25 %. The fermentation was conducted in the similar manner to those mentioned in 3.4.2 while the optimal C/N ratio of the production

medium which obtained from 3.4.2.1 was use. Samples were collected every 12 h throughout the cultivation for analyses of the remaining glucose, nitrogen, itaconic acid, and other byproducts.

3.4.2.3 Gene expression of the key enzymes responsible for itaconate production

To better understand the regulation of the genes responsible for itaconic acid production under the optimized condition, the fermentation sample at the end of the growth phase and those during the production phase were collected for RNA extraction, subsequent transcriptome sequencing and differential expression analysis.

3.4.2.3.1 Complementary DNA library preparation and transcriptome sequencing

Barcoded RNA libraries were prepared using Lexogen's Quant-Seq 3' mRNA seq kit for Ion Torrent (Lexogen, Vienna, Austria). This approach generated the libraries of the sequences close to the 3' end of the polyadenylated RNAs and only one fragment was produced per transcript. The RNA input was quantified by the spectrophotometry or the fluorometry. Approximately 300-500 ng of the RNA input was required for the library generation. The modified Quant-Seq protocol was performed as suggested for the low input, partially degraded RNA. The External RNA Controls Consortium (ERCC) obtained from Life Technologies (Carlsbad, CA, USA) were used to spike into each of the prepared library reactions at the manufacturer's recommended concentration. The library quantification and quality control were performed using high sensitivity DNA kit and Agilent 2100 Bioanalyzer (Agilent, Santa Clara, CA, USA).

The DNA templates for sequencing were prepared using 200 bp v3 OT2 kit and the Ion One Touch 2 platform (Life Technologies). Sequencing was performed on the Ion Proton with the signal processing and basecalling using Ion Torrent Suite v5.0.4 (Life Technologies). Raw sequence from each sample was uploaded to Partek Flow. Adapter sequences were trimmed. Bases were then trimmed accordingly to the visual representation and quality score to size below 170 bp. The resulting reads were then aligned to *A. terreus* NIH2624 genome references downloaded from http://fungi.ensembl.org/info/website/ftp/index.html using Star 2.4.1d. Transcript quantification was performed using the Partek E/M method available in Partek Flow.

3.4.2.3.2 Analyses of transcriptomes

The sequences of the adapters including TGGAATTCTCGGGTG, CACCCGAGAATTCCA, AATCTCGTATGCCGTCTTCTGCTTGC, AGATC GGAAGAGCTCGTATGCCGTCTTCTGCTTG, AGATCGGAAGAGCGTCGTGT AGGGAAAGAGTGT, AGATCGGAAGAGCGGTTCAGCAGGAATGCCGAG. The sequence alignment with *A. terreus* NHI2624 (assembly ASM14961v1) genome was performed using STAR v2.4.2a. Samtools v0.1.19-96b5f2294a was used with the default setting to generate the bam index files. Quantification of the gene expression was performed by Htseq v0.6.0 with –f and –s options indicating bam inputs and un-stranded reads, respectively. Cuffdiff v2.1.1 was used to estimate transcript abundance with the --no-diff and default options to generate the differential analysis files for each of the described comparisons.

3.4.3 Sample analyses and calculations

Cell growth and product formation during the fermentation were determined. The product yield was calculated from the ratio of the product formed to the amount of glucose consumed. The volumetric productivity was defined as the total amount of the product formed per unit volume per time.

3.4.3.1 Cell biomass

Cell biomass concentration was determined from the cell dry weight. The collected fermentation sample was filtered through the Whatman filter paper No.4 to harvest the cell biomass. The cell biomass was thoroughly rinsed with the deionized water and then dried at 80 °C until constant dry weight (DW) was obtained. Cell concentration (in g/L) was calculated by

$$\text{Cell concentration } (\frac{\text{g}}{\text{L}}) = \frac{\text{Cell dry weight on filter paper (g)} - \text{dry weight of filter paper (g)}}{\text{Fermentation broth volume (L)}}$$

3.4.3.2 Remaining glucose and fermentation products

The fermentation broth was centrifuged at 10000 *g* for 7 min. The supernatant was collected for analyzing the remaining glucose, itaconic acid, and other byproducts by High Performance Liquid Chromatography (Shimadzu 10Ai). The sample was diluted and filtered through the hydrophilic PTFE membrane. The particle-free sample (15 μL) was automatically injected into an organic acid column (Biorad, Aminex HPX-87H ion exclusion organic acid column; 300 mm × 7.8 mm) maintained at 45 °C in a column oven. Sulfuric acid (0.4 mM) was used as the mobile phase at the flowrate of 0.4 mL/min. A refractive index detector was used to detect the organic compounds, e.g.,

glucose, itaconic acid, citric acid, cis-aconitic acid, succinic acid, oxaloacetic acid, L-malic acid, pyruvic acid, formic acid, and ethanol present in the sample. The standards containing 0-2 g/L of each compound previously mentioned were injected as the references to determine the concentration of each compound in the sample. The chromatogram peak area was selected for the comparison basis.

3.4.3.3 Ammoniacal nitrogen analysis

The residual ammoniacal nitrogen was determined by Indophenol blue method (Tzollas et al., 2010). Before assay, the following reagents were prepared accordingly. 1) Phenol-alcohol solution was prepared from dissolving 10 g phenol (reagent grade) into 100 mL ethanol (95 %v/v). 2) 0.5 % sodium nitroprusside was prepared by dissolving 1 g sodium nitroprusside into 200 mL water. 3) Alkaline solution was prepared by dissolving 100 g trisodium citrate and 5 g sodium hydroxide into 500 mL water. 4) Sodium hypochlorite solution was prepared from the commercial hypochlorite (Chlorox). 5) Oxidizing solution was prepared in the same day before use from a mixture of 100 mL sodium citrate solution and 25 mL hypochlorite solution. The reaction assay was started by adding 500 µL sample into the mixture of phenol solution (20 µL), sodium nitroprusside solution (50 µL), and oxidizing solution (125 µL). The reaction was developed for 1 h under darkness. The optical purity of the mixture was measured at the wavelength of 640 nm and the ammonia concentration in the sample was calculated from the standard curve.

3.4.3.4 Phosphate analysis

The residual phosphate was determined by malachite green method (Baykov et al., 1988). The dye solution was prepared before assay by adding 60 mL concentrated

sulfuric acid. To 300 mL water. The solution was allowed to cool down to room temperature before 0.44 g malachite green was supplemented. The orange solution was then prepared on the same day before use from mixing 2.5 mL ammonium molybdate (7.5 %) and 0.2 mL tween 20 (11%) into 10 mL dye solution. For the reaction assay, 100 µL of sample were mixed with 400 µL orange solution. The absorbance at 630 nm was read within 10 min after mixing. The phosphate concentration in the sample was calculated from the standard curve.

CHAPTER 4

RESULTS AND DISCUSSION

4.1 Regulating pyruvate carboxylase in the living culture of *Aspergillus terreus* NRRL1960 by L-aspartate

4.1.1 Glucose-based fermentation without L-aspartate of *A. terreus* NRRL1960 in flask fermentation (Control)

4.1.1.1 Fermentation profile of glucose-based fermentation of *A. terreus* NRRL1960 in flask fermentation

The fermentation kinetics of *A. terreus* NRRL1960 grown in 2 phases for itaconic acid production shows in Figure 4.1. Unlike other itaconic acid fermentation processes reported elsewhere in the literatures, 2-phase fermentation was employed to achieve high cell density during the growth phase by growing *A. terreus* in the rich medium containing organic nitrogen source with the subsequent itaconic acid production by the high cell density using other medium compositions that promoted itaconic acid synthesis. During the growth phase, cell biomass was built up rapidly (8.96 g/L with 1.34 g cell per gram glucose consumed and 0.19 g cell/L/h) while there was no itaconic acid produced.

After 48 h, the growth medium was discarded and the culture was filled up with the production medium containing $(NH_4)_2SO_4$ as the sole nitrogen source at the high C/N weight ratio of 42:1. Increasing cell biomass production was continuously

observed at the slightly lower rate compared to that during the growth phase until 120 h (red line). When changing the medium, inorganic nitrogen ($(NH_4)_2SO_4$) with the supplemented phosphate in KH_2PO_4 in the production medium maintained the growth of *A. terreus*; however, at a lower rate compared to that cultivated in the growth medium with yeast extract.

The lower growth rate confirmed the evidence of the lower ATP regeneration due to limited phosphate pool; thus, the regeneration process occurred by substrate level phosphorylation rather than oxidative phosphorylation. At 120 h, itaconic acid was firstly observed in the fermentation broth. Later, the growth rate was dropped while glucose consumption rate remained constant and itaconic acid was produced at the constant rate (0.16 g/L/h).

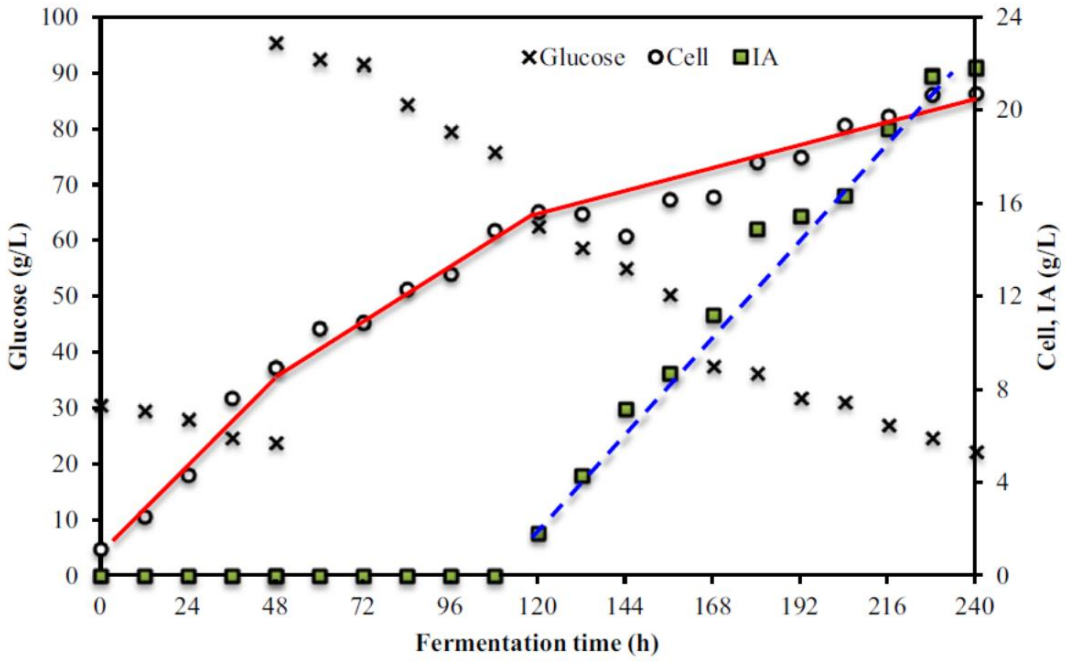

Figure 4.1 Fermentation kinetics of *A. terreus* NRRL1960 grown in glucose-based medium in the shake flask culture. Fermentation consisted of two phases. The growth phase took 48h where yeast extract was used as a sole nitrogen source. The growth medium was replaced by the production medium containing the inorganic nitrogen source after 48 h. The fermentation was prolonged until 240 h. The red trend lines indicate two growth rates of *A. terreus* during cultivation. The corresponding blue trendline indicates itaconic acid production during the slow growth.

4.1.1.2 Key enzymes responsible for itaconic acid synthesis

To better understand the synthesis of itaconic acid by *A. terreus* during 2-phase fermentation cultivation, the activity of the key enzymes related in itaconic acid production was assayed (Figure 4.2).

(a)

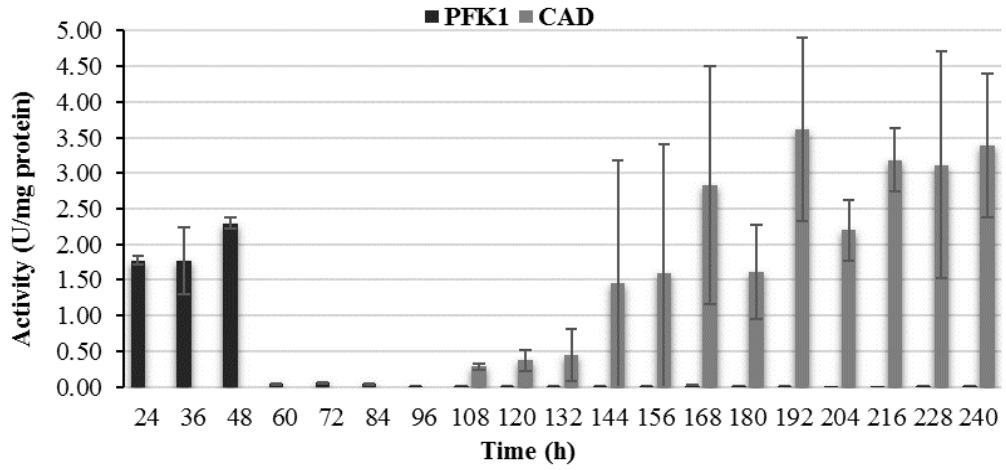

(b)

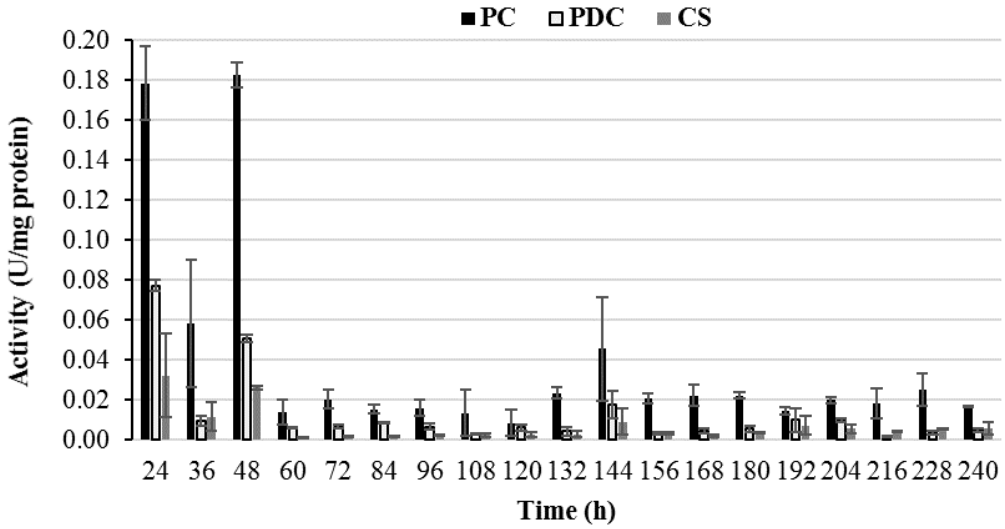

Figure 4.2 Key responsible enzymes in itaconic acid production by *A. terreus*. The specific activity of the enzymes was assayed from the collected fermentation samples during cultivation of *A. terreus* in the glucose-based medium in 2-phase fermentation. Enzyme assay was carried out after 24-h cultivation when sufficient cell biomass was produced. The high expression levels of PFK and CAD were observed (more than ×20 larger) (a) compared to those of PC, PDC, and CS, the key intermediate enzymes in TCA cycle (b)

During the growth phase, the specific activity of PFK was approximately 2 U/mg protein while later in the production phase, the PFK-specific activity dramatically dropped (Figure 4.2(a)). This was presumably due to the change in medium compositions from organic to inorganic nitrogen for slight cell growth and maintenance during the production phase. It was claimed that a univalent cation such as NH_4^+ had a role in PFK regulation as it might provoke inhibition by citrate in vivo (Tevz et al., 2010). Subsequently, the increasing activity of CAD (Figure 4.2(a)) and the accumulation of itaconic acid (Figure 4.1) were observed with the lowered PFK activity during the production phase. When growing *A. terreus* using yeast extract under sufficient oxygen supply, glucose was rapidly metabolized in to pyruvate through the Embden-Meyerhof Parnas (EMP) pathway. Pyruvate was then either transported to the mitochondria and later converted into acetyl CoA or carboxylated into oxaloacetate (OAA) in the cytosol (Klement and Buchs, 2013). Completed TCA cycle coupling with an electron transport chain (ETC) resulted in cell biomass and a large amount of ATP generation (Huang et al., 2014; Zhou et al., 2009).

Changing the medium to the production medium containing a small amount of $(NH4)_2SO_4$ as well as decreasing the initial pH to 2.0 caused the lowered PFK activity due to lower oxygen solubility at low pH and the stimulated citrate inhibition of PFK by $NH4^+$. In order to balance citrate flux in the mitochondria compartment under nitrogen limitation so that glucose flux towards the glycolysis could proceed, OAA in the cytosol was converted to malate, which was transported into the mitochondria by malate/citrate antiporters. In the mitochondria, acetyl CoA and OAA were irreversibly condensed into citric acid by CS. Citric acid was then reversibly converted to isocitrate and cis-aconitate by aconitase (ACO). Cis-aconitate was transported back to the cytosol

using mitochondrial tricarboxylic transporter (MttA) and then decarboxylated into itaconic acid by CAD (Figure 4.3) (Steiger et al., 2013). The increasing CAD activity during the production phase was the evidence of MttA function in order to lower citrate isomer in the mitochondria thus glycolytic flux could be still driven towards pyruvate (Figure 4.2(a)).

Similarly, the specific activities of PC, PDC, and CS were high during the growth phase. This confirmed the high level of the oxidative phosphorylation in *A. terreus* with sufficient oxygen supply and rich nitrogen source (Figure 4.2b).

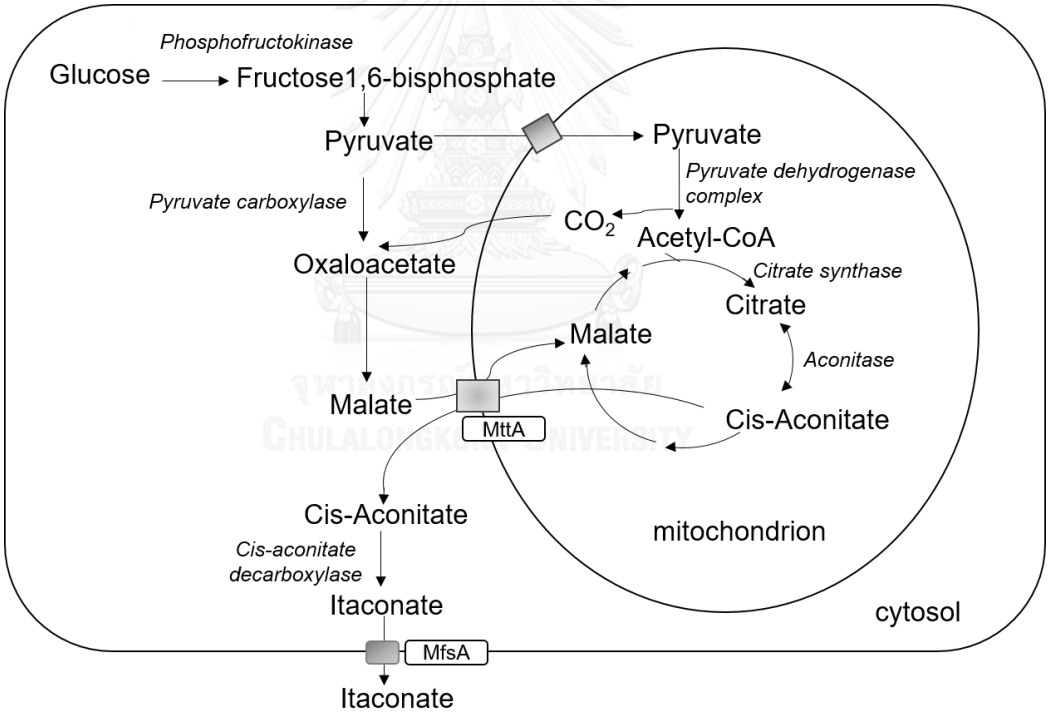

Figure 4.3 Biosynthesis pathway of itaconic acid in *A. terreus*. Malate/citrate transport during nitrogen limitation played role controlling itaconic acid synthesis. (Modified from Steiger et al. (2013)).

In this study, further growth was observed after changing the medium to the production medium (Figure. 4.1) while the activity of PFK, PC, PDC, and CS dramatically dropped (Figure. 4.2). This rather implied ATP conservation process instantaneously occurred at the beginning of the production phase when phosphate became limited. Nonetheless, as observed from the expression level of CAD, itaconic acid production started later at 120 h under both phosphate and nitrogen limitation condition (Riscaldati et al. 2000). To immediately initiate itaconic acid synthesis in 2-phase fermentation process after changing to the production medium, not only balancing the ratio of C/N/P in the medium is necessary, in term of the biosynthesis flux, the rate of OAA/acetyl CoA formation, citrate isomerization, and malate/cis-aconitate transport must be balanced while ATP regeneration must be also regulated (Figure 4.3).

4.1.2 Effect of L-aspartate on glucose-based fermentation with various concentration of *A. terreus* NRRL1960 in flask fermentation.

4.1.2.1 Effect of L-aspartate on metabolism of *A. terreus* during growth phase

To investigate the metabolic response of *A. terreus* on medium change during 2-phase fermentation, L-aspartate was added into the fermentation medium. Figure 4.4 shows the morphology of *A. terreus* grown in the glucose-based medium containing L-aspartate. It is clear that the morphology changed with the presence of L-aspartate. Smaller pellets were obtained when the concentration of L-aspartate was increased in the growth medium. Cell biomass production was also lower with the increasing L-aspartate concentration (Table 4.1). The specific activity of the key enzymes involving

in biosynthesis confirmed the evidence of PC feedback inhibition by L-aspartate (Figure 4.5). Lower PFK activity (Figure 4.5(a)) was found with the increasing L-aspartate concentration in the growth medium. This was apparently due to the fact that L-aspartate triggered PC by binding at its allosteric site; thus, limiting PC action (Figure 4.5(b)) and consequently reducing pyruvate flux towards OAA and malate. This eventually led to the reduction in biomass synthesis (Myers et al., 1983; Zeczycki et al., 2010).

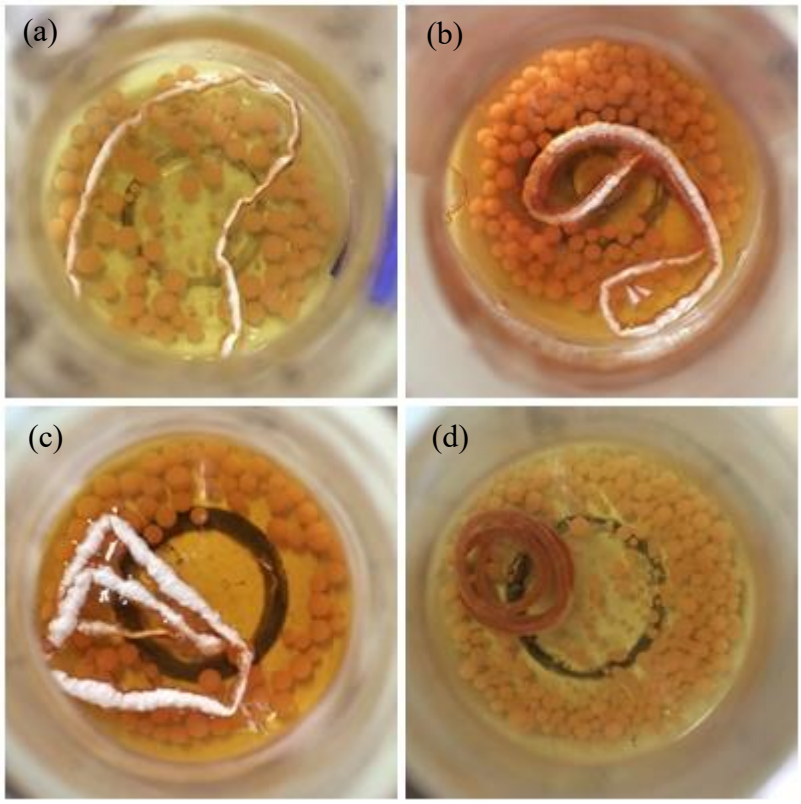

Figure 4.4 Morphology of *A. terreus* cultivated in the growth medium containing L-aspartate. a control (no L-aspartate). b 0.1 mM L-aspartate. c 1.0 mM L-aspartate. d 10.0 mM L-aspartate

Table 4.1 Cell biomass production during the growth phase of 2-phase fermentation of *A.terreus* for itaconic acid synthesis

L-aspartate (mM)	Cell biomass production during the growth phase		
	Final conc. at 48 h (g/L)	Yield (g/g glucose consumed)	Productivity (g/L·h)
0 (control)	8.96±3.02	1.12	0.17
0.1	5.32±0.34	1.39	0.09
1.0	6.96±0.45	1.13	0.13
10.0	2.31±0.11	0.21	0.03

L-aspartate at different concentration was added into the glucose-based growth medium. The fermentation was carried out at 30 °C and 200 rpm in a shaken flask. The initial pH was 3.0

(a)

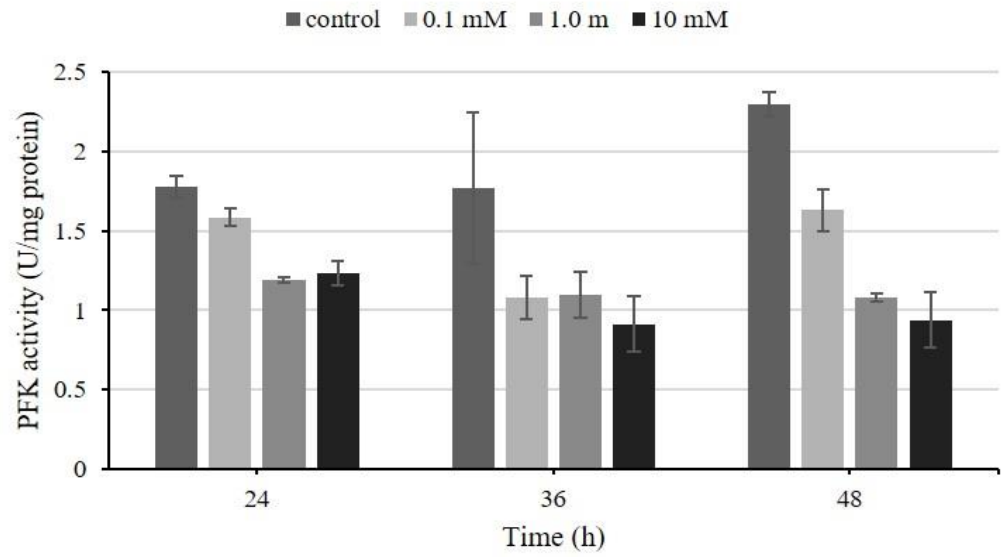

(b)

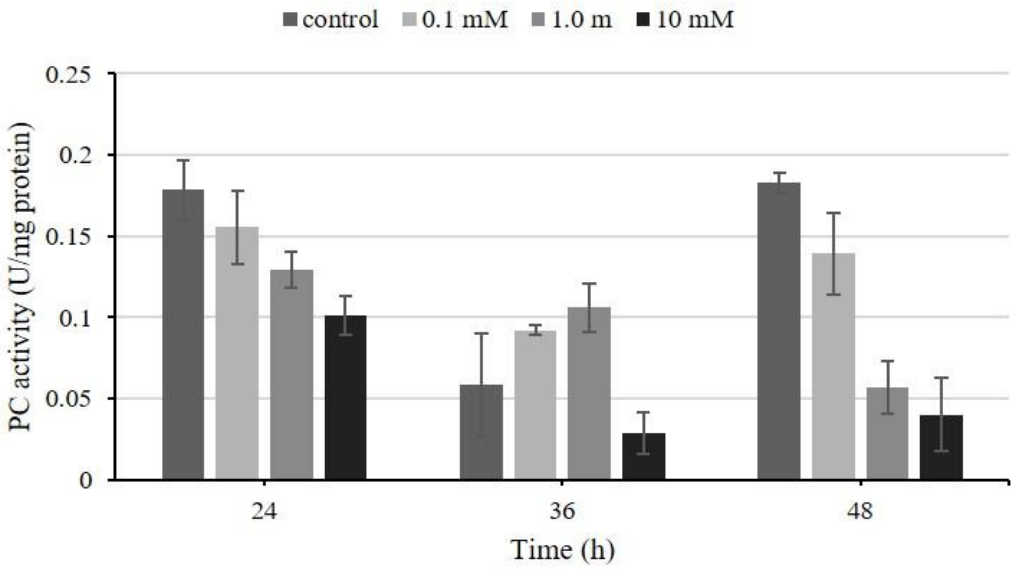

Figure 4.5 The metabolic response of *A. terreus* when L-aspartate, the allosteric PC inhibitor was present during the growth phase. Key enzymes responsible for growth and ATP regeneration including PFK (a) and PC(b) were observed for their changes of activities when PC inhibitor was present.

4.1.2.2 Effect of L-Aspartate on metabolism of *A. terreus* during production phase

Most PCs have an α4 quaternary structure with the four identical subunits containing a biotin carboxylase (BC) domain, a carboxyl transferase (CT) domain, and a biotin carboxyl carrier protein (BCCP) domain. The α4 PCs are commonly activated by acetyl CoA (Adina-Zada et al., 2012).

From the above-mentioned claim and the metabolic response of *A. terreus* to L-aspartate during the growth phase, L-aspartate was introduced into the pregrown culture of *A. terreus* during the production phase. Increasing the concentration of L-aspartate up to 10.0 mM improved itaconic acid production (Figure 4.6). Not only the higher titer could be achieved, but also sufficient amount of L-aspartate shortened the lag time before itaconic acid production after changing the medium. Nonetheless, excess L-aspartate somewhat caused the adverse effect on itaconic acid production when 100.0 mM was added into the production medium (Table 4.2). PC was strongly inhibited at 100.0 mM L-aspartate as it competitively bound at its active site preventing the conversion of pyruvate to OAA and subsequently to malate. The lowered malate pool reduced the transport fluxes between malate and cis-aconitate, the CAD substrate for itaconic acid via the malate/cis-aconitate antiporter (Figure 4.3). At the same time, the large pool of acetyl CoA induced citrate formation. When high citrate concentration was present, it eventually inhibited PFK in glycolysis. This consequently slowed down the metabolism of *A. terreus* as observed from the prolonged turnover time of 120 h for itaconic acid production. As a result, itaconic acid production dropped when 100.0 mM L-aspartate was present in the production medium.

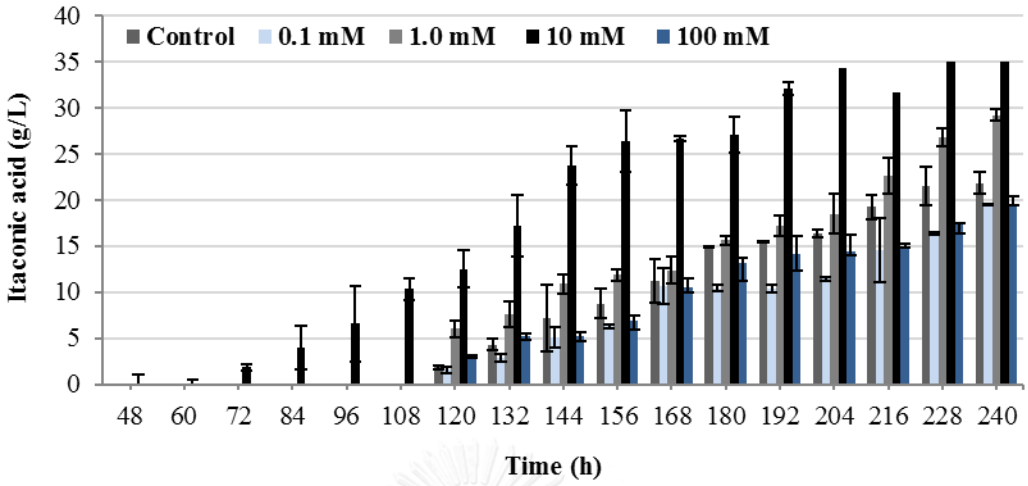

Figure 4.6 Itaconic acid accumulation during the production phase of 2-phase fermentation of *A. terreus* in the glucose-based media containing an allosteric acetyl CoA inhibitor (L-aspartate) at different concentrations. *A. terreus* was pregrown in the growth medium and later, it was added into the culture during the production phase. Control represented the fermentation without L-aspartate

Table 4.2 Fermentation performance of *A. terreus* during the production phase with the presence of PC allosteric inhibitor, L-aspartate

Itaconic acid production	**L-aspartate concentration**				
	Control[c]	0.1 mM	1.0 mM	10.0 mM	100.0 mM
Final conc. (g/L)	21.80±1.17	19.45±0.04	29.14±0.65	34.95±0.70	19.49±0.10
Yield (g/g)	0.43±0.00	0.34±0.01	0.36±0.01	0.47±0.05	0.25±0.02
Productivity (g/L·h)	0.17±0.00	0.14±0.01	0.19±0.01	0.19±0.01	0.14±0.01
Time started to produced (h)[a]	120	120	120	72	120
Time reached highest concentration (h)[b]	240	240	240	240	240

a Total time (started from growth phase of 48 h and prolonged production phase) until itaconic acid was produced

b Total time (started from growth phase of 48 h and prolonged production phase) until the highest itaconic acid concentration was achieved

c Fermentation without L-aspartate (control fermentation)

From the concentration of L-aspartate studied, 10.0 mM gave the well-optimized condition that promoted itaconic acid synthesis. Approximately one third shorter lag time was achieved at this concentration of L-aspartate present in the fermentation. While the production yield reached up to 65 % of the theoretical yield (0.72 g/g) compared with that obtained from the control fermentation (60 %) (Table 4.2).

The expression of PC confirmed the evidence of improved itaconic acid fermentation (Figure 4.7(a)). Dramatically decreasing PC activity was observed

resulting in lowered OAA in the cytosol. Subsequently, malic acid concentration was decrease in the cytosol. Malate/citrate antiporters subsequently drove the transport of cis-aconitate to the cytosol so that the malate could be transported into the mitochondria in response to the living *A. terreus* to complete TCA cycle. The presence of cis-aconitate in the cytosol-induced CAD as observed from the increasing activity of this enzyme (Figure 4.7(b)) and itaconic acid formation; after 24 h, the production phase started (Figure 4.6) while the control fermentation required up to 72 h for itaconic acid production firstly observed (Figure 4.6). The flux of citrate towards cis-aconitate and the transport of malate/citrate antiporters induced the activities of CS and PFK (Figure 4.7(c), 4.7(d)). CAD further converted cis-aconitate, citrate isomer, into itaconic acid to balance the metabolic fluxes. This eventually resulted in the improved itaconic acid yield (0.47 g/g) of 8.33 % and final concentration (34.95 g/L) of 60.32 % compared to those obtained from the control fermentation (0.43 g/g and 21.80 g/L, respectively).

(a)

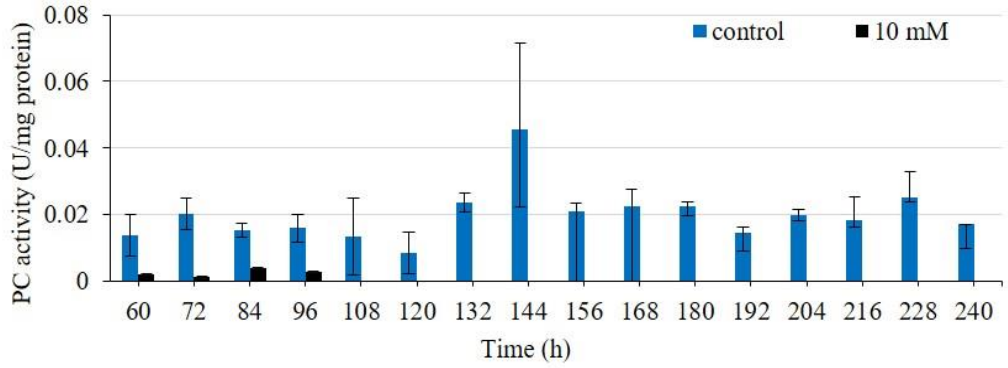

(b)

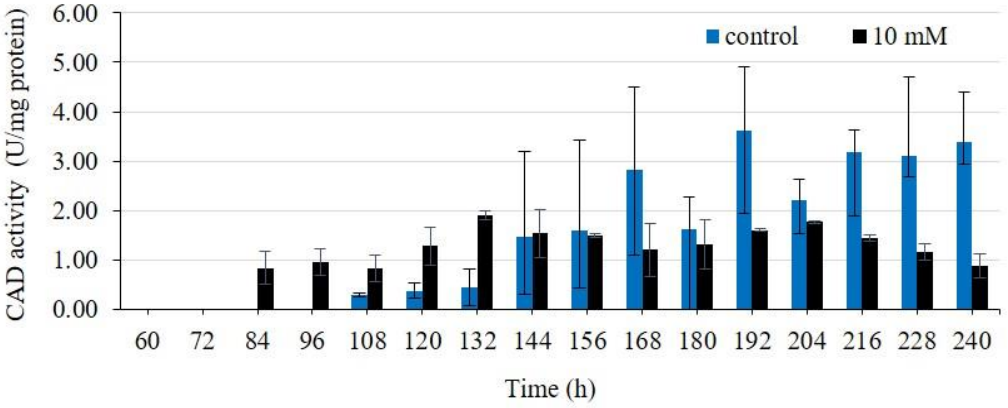

(**c**)

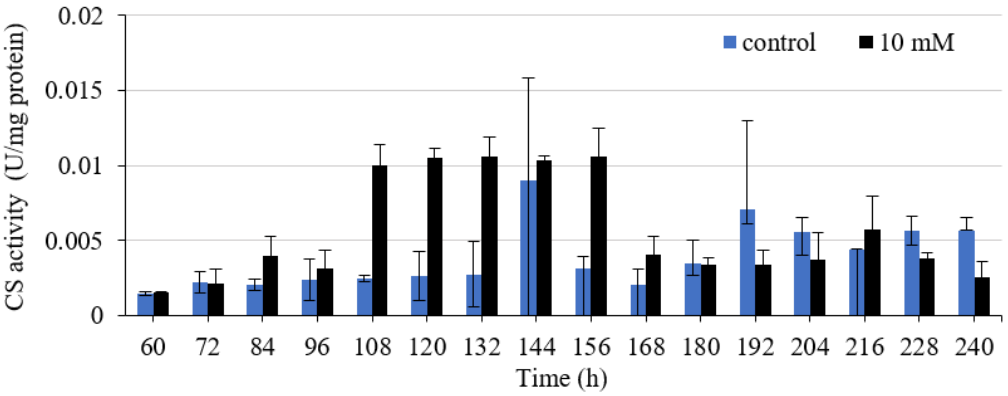

(**d**)

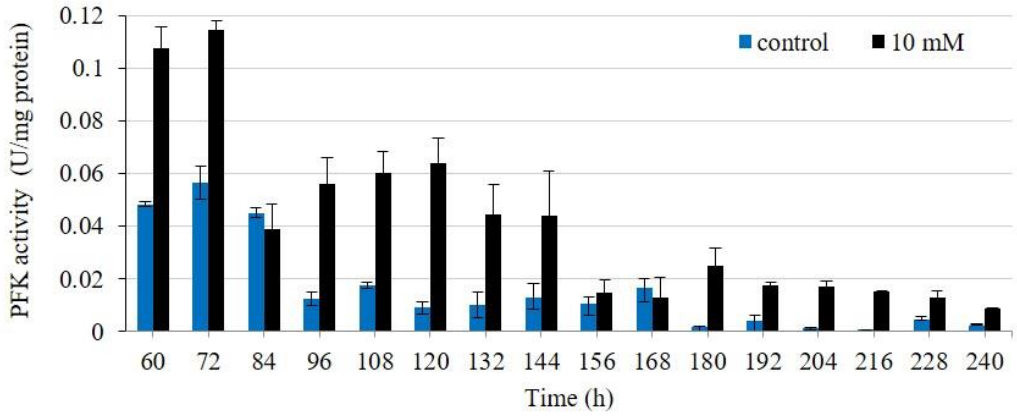

Figure 4.7 Specific activities of the key responsible enzymes in itaconic acid production by *A. terreus* when L-aspartate, the allosteric PC inhibitor was present at 10.0 mM during the production phase in 2-phase fermentation

As aforementioned, L-aspartate played a role in allosteric inhibition of PC in the living culture of *A. terreus*. This resulted in metabolic flux shift towards itaconic acid production. The incomplete TCA cycle with the enhanced PFK activity revealed that TCA intermediates were bypassed towards itaconic acid as the result of PC inhibition and ATP conservation by the well-optimized concentration of allosteric PC inhibitor, L-aspartate, during the production phase with the limited growth of *A. terreus* (Li et al. 2011). Moreover, the finding of fermentation profile of *A. terreus* NRRL1960 in flask fermentation indicated growth-limiting condition was necessary for itaconic acid synthesis (Figure 4.1). Similar growth pattern of *A. terreus* NRRL 1960 was observed by Riscaldati et al. (2000). The evidence of phosphate and nitrogen limitation led to the accumulation of itaconic acid. The results show in Figure 4.1 and those in Riscaldati et al. (2000) revealed that the fermentation exhibited mixed-growth associated product formation kinetics (Riscaldati et al., 2000). Nonetheless, from the

kinetics model non-growth condition did not give the better itaconic acid production. With the proper N/P ratio in the production medium and other key controlling factors, it is believed that itaconic acid production can be further improved in 2-phase fermentation in the stirred-tank bioreactor.

Therefore, to better control better control of growth and product formation. and understand itaconic acid biosynthesis pathway by *A. terreus*, 2-phase fermentation process was conducted and the effects of key controlling factors including C/N ratio, dissolved oxygen, and pH on metabolic response and itaconic acid production were elucidated in the next experiment.

4.2 Process optimization in 2-phase fermentation in the stirred-tank bioreactor for itaconic acid production by *A. terreus* NRRL1960

4.2.1 Effect of C/N ratio on the metabolic behavior of *A. terreus*

Figure 4.8 shows the fermentation kinetics of *A. terreus* cultivated in the production medium with the varied C/N ratios. It was found that no itaconic acid production when nitrogen was absent from the production medium (Figure 4.8 (a)). Cell growth was prolonged after the growth phase from 48 h until 84 h then stopped. Glucose was slowly consumed along the cultivation. Ethanol was observed after 144 h indicating the anaerobic alcohol fermentative pathway was activated although the dissolved oxygen was maintained at 20 % DO.

The C/N ratio of 100/1.18 resulted in itaconic acid production with less cell biomass production. itaconic acid production appeared after 120 h after ammonium and phosphate were limited (Figure 4.8(b)). Cell biomass production was continued only a

short period (from 48 to 60 h) then the cell concentration rather remained constant. Glucose was continuously consumed at the lower rate than that observed from the fermentation without nitrogen.

The highest itaconic acid production of 10.40 g/L at 240 h was observed at the C/N ratio of 100/2.36 with the presence of formate as a major byproduct (Figure 4.8(c)). Also, the improved itaconic acid yield approaching 60 % of the theoretical yield (0.72 g/g) was obtained. Although it was attempted to limit growth during the production phase, nitrogen was still required. When nitrogen was absent, no itaconic acid production was observed. Papagiani et al. (2005) revealed that a high intracellular ammonium concentration could prevent the inhibition of phosphofructokinase that subsequently converted glucose and fructose to pyruvate (Papagianni et al., 2005). When ammonium was present, the enzyme could effectively work that eventually led to the enhanced glycolytic fluxes towards pyruvate, the key intermediate.

Further decreasing the C/N ratio to 100/3.54 gave the negative effect on itaconic acid production. About half of itaconic acid was produced at this C/N ratio compared with that at the ratio of 100/2.36. The final concentration of formate was also reduced (3.17 g/L at 240 h). Compared with other C/N ratios studied, the highest glucose consumption rate was observed at this C/N ratio (Figure 4.8(d)). Increasing the nitrogen content in the medium, on the other hand, resulted in the lower itaconic acid production with the absence of formate but ethanol appeared late (after 216 h) (Figure 4.8(e)).

(a)

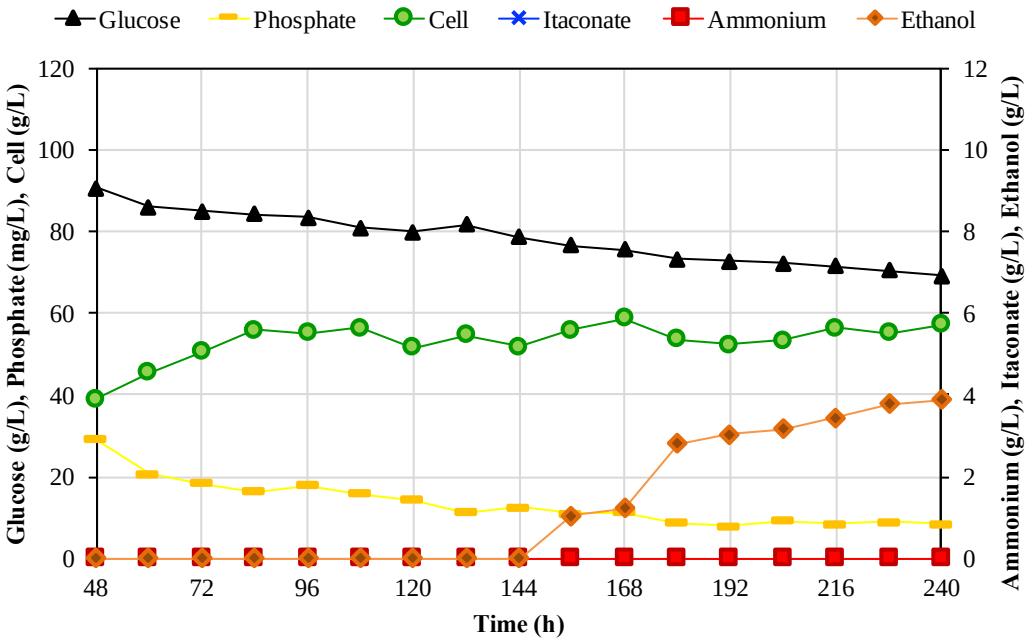
Glucose
Phosphate
Cell
Itaconate
Ammonium
Ethanol
Glucose (g/L), Phosphate (mg/L), Cell (g/L)
Ammonium (g/L), Itaconate (g/L), Ethanol (g/L)
Time (h)
0
20
40
60
80
100
120
0
2
4
6
8
10
12
48
72
96
120
144
168
192
216
240

(b)

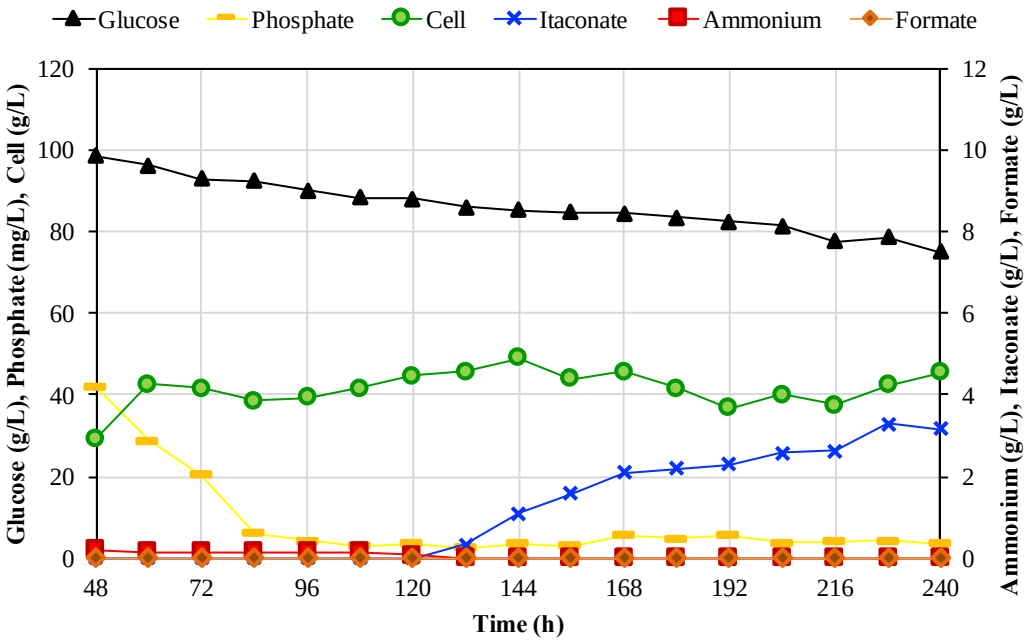
Glucose
Phosphate
Cell
Itaconate
Ammonium
Formate
Glucose (g/L), Phosphate (mg/L), Cell (g/L)
Ammonium (g/L), Itaconate (g/L), Formate (g/L)
Time (h)
0
20
40
60
80
100
120
0
2
4
6
8
10
12
48
72
96
120
144
168
192
216
240

(c)

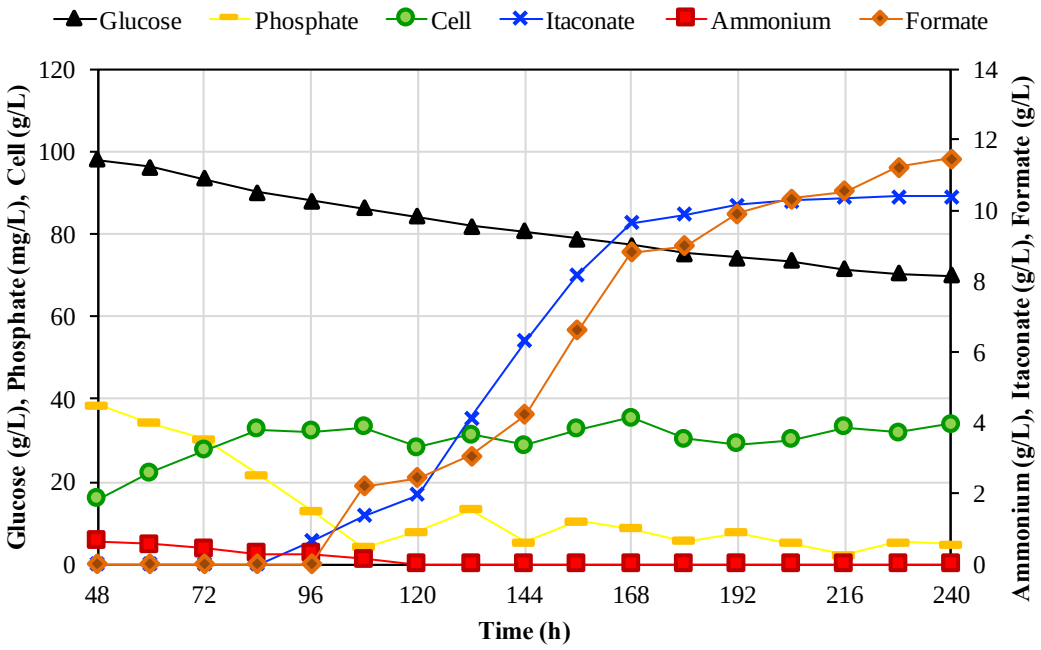
Glucose
Phosphate
Cell
Itaconate
Ammonium
Formate
Glucose (g/L), Phosphate (mg/L), Cell (g/L)
Ammonium (g/L), Itaconate (g/L), Formate (g/L)
Time (h)
0
20
40
60
80
100
120
0
2
4
6
8
10
12
14
48
72
96
120
144
168
192
216
240

(d)

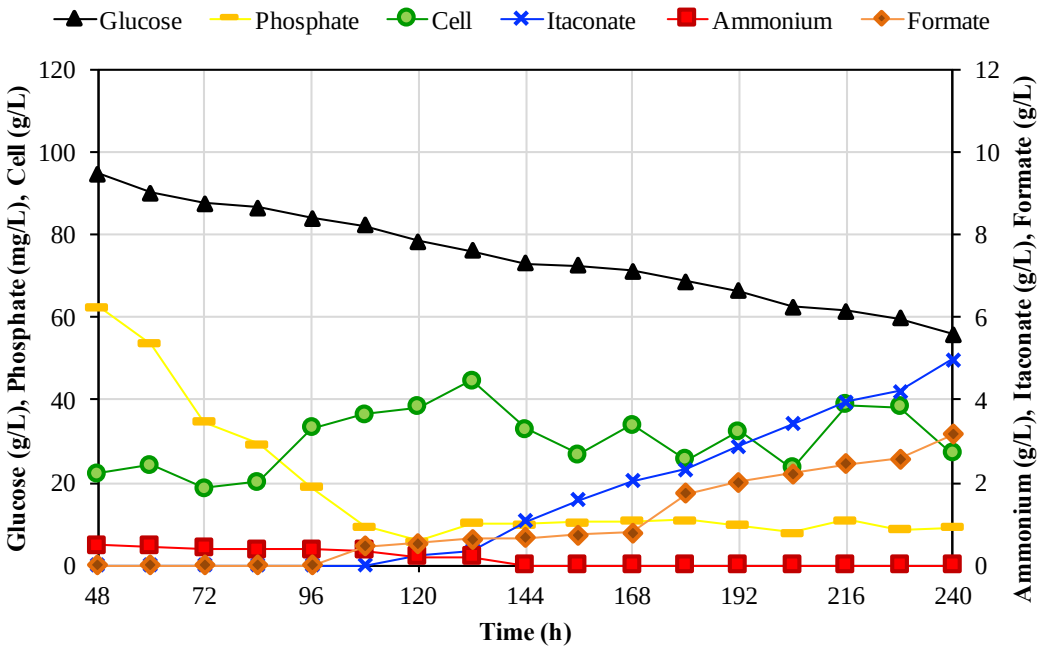
Glucose
Phosphate
Cell
Itaconate
Ammonium
Formate
Glucose (g/L), Phosphate (mg/L), Cell (g/L)
Ammonium (g/L), Itaconate (g/L), Formate (g/L)
Time (h)
0
20
40
60
80
100
120
0
2
4
6
8
10
12
48
72
96
120
144
168
192
216
240

(e)

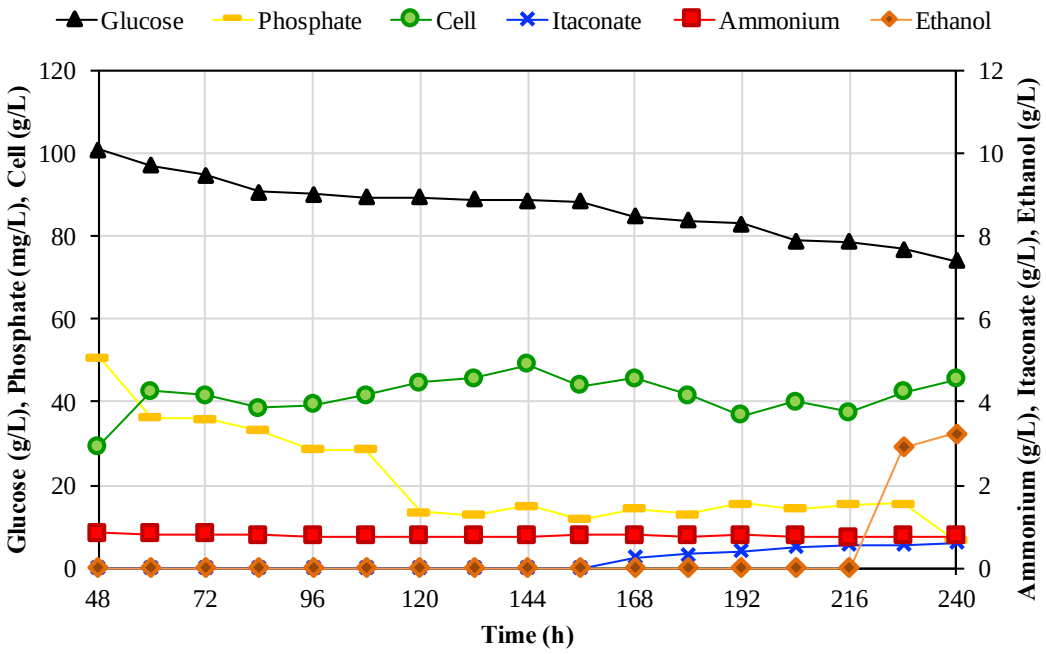

Figure 4.8 Kinetics profiles of *A. terreus* cultivated in the production medium with varied C/N weight ratios, e.g., (a) 100/0, (b) 100/1.18, (c) 100/2.36, (d) 100/3.54, (e) 100/4.72. The bioreactor was controlled at 30 °C, 100 rpm, 20 %DO, and pH 2.00.

With the optimized C/N ratio, itaconic acid was found in the fermentation at 96 h when the concentrations of ammonium and phosphate became low at 0.29 g/L and 13.0 mg/L, respectively (Figure 4.8(c)). It was claimed that both nitrogen and phosphate limitation were essential for itaconic acid production as the growth was limited (Boer et al., 2010; Papagianni et al., 2005). This finding was consistent with our previous study indicating that itaconic acid was firstly observed in the fermentation broth when the growth stopped (See in 4.1.1) (Songserm et al., 2015). Klement and Buchs (2013) also reported that the overproduction of itaconic aci required nutrient limitation for uncoupled glycolysis and oxidative phosphorylation (Klement and Buchs, 2013).

Riscaldati et al. (2000) found that itaconic acid was started to secrete into the fermentation broth when the phosphate concentration in the medium dropped to approximately 10 mg/L with the continuously decreasing nitrogen concentration from 20 mg/L to less than 1 mg/L while the cell concentration was slowly increased from 3 g/L to 10-11 g/L (Riscaldati et al., 2000). Hevekerl et al. (2014a) claimed that under the optimized operating condition, itaconic acid was produced after 1-day cultivation when the phosphate concentration was decreased (Hevekerl et al., 2014a). At this C/N ratio, itaconic acid production appeared at 96 h while formate was formed at 108 h. It was observed that itaconic acid was produced after the cell growth was stopped; thus, confirming that itaconic acid production by *A. terreus* during the production phase followed the non-growth associated product kinetics model.

Although the C/N ratio of 100/2.36 gave the highest itaconic acid production in term of product concentration and yield compared with the other C/N ratios studied, the productivity was still low (Table 4.3). Along with a large amount of formate present, this revealed that the process conditions employed might not be well optimized for *A. terreus* to utilize glucose for itaconic acid.

Table 4.3 Fermentation kinetics of *A. terreus* cultivated during the production in the medium with the varied C/N ratio. The bioreactor was controlled at 30 °C, 100 rpm, 20% DO, and pH 2.0.

C/N ratio	Final itaconate (g/L)	Itaconate yield (g/g)	Itaconate productivity (g/L·h)	Glucose consumption (g/L·h)
100/0	0	0	0	0.10
100/1.18	3.70±0.74	0.25	0.03	0.10
100/2.36	10.40±0.03	0.43	0.07	0.15
100/3.54	4.97±2.06	0.22	0.04	0.18
100/4.72	0.62±0.27	0.05	0.01	0.12

4.2.2 The metabolic response of *A. terreus* on DO and pH during the production phase

Unlike those claimed in the 1-phase fermentation for itaconic acid production, we observed that low dissolved oxygen enhanced itaconic acid production during the production phase in the 2-phase fermentation process. While, increasing the DO level lowered itaconic acid production during the production phase in the 2-phase fermentation process applied in this study (Table 4.4).

It was observed that the DO level controlled by varied air flowrate affected the morphology of *A. terreus* throughout the fermentation when the agitation rate was fixed at 100 rpm to avoid rigorous shear damage by mixing. Different controlled DO levels

resulted in the different morphological forms (Figure 4.9). More dispersed mycelia were observed in the fermentation broth under the controlled DO of 20 % while more mycelial clumps were obtained at 10 %DO. Previous studies reported that the production of itaconic acid was correlated with the correct morphological form. In 1995, Gyamerah reported that the high itaconic acid concentration was obtained with the small and tense mycelial pellets (Gyamerah, 1995). In 2014, Gao et al. reported that with the mycelial clumps the highest itaconic acid production was obtained in comparison with the pellets and the dispersed mycelia (Gao et al., 2014).

Table 4.4 Effect of pH and DO level on *A. terreus* cultivated in the production medium with the C/N ratio of 100/2.36 at 30 °C, 100 rpm.

%DO	pH	Itaconate				Cell		Formate		Ethanol	
		Final conc. (g/L)	Yield (g/g)	Productivity (g/L·h)	Produced at (h)	Final conc. (g/L)	Yield (g/g)	Final conc. (g/L)	Yield (g/g)	Final conc. (g/L)	Yield (g/g)
10	1.85	22.37	0.49	0.16	108	64.40	0.51	6.30	0.12	1.95	0.04
	2.00	35.65	0.52	0.26	108	50.00	0.15	8.70	0.12	0	0
	2.15	22.39	0.48	0.15	96	46.60	0.16	9.42	0.17	0	0
	2.30	15.86	0.38	0.13	108	60.20	0.42	8.00	0.13	0	0
15	1.85	23.28	0.47	0.19	132	44.60	0.31	4.70	0.08	1.95	0.03
	2.00	22.85	0.40	0.20	120	54.00	0.20	5.43	0.08	0	0
	2.15	8.37	0.23	0.06	132	60.50	0.25	3.18	0.07	0	0
	2.30	8.14	0.25	0.05	132	54.70	0.35	2.22	0.05	3.14	0.07
20	1.85	14.73	0.33	0.07	132	43.00	0.15	5.84	0.10	0	0
	2.00	12.19	0.28	0.08	120	52.00	0.22	6.09	0.09	0	0
	2.15	4.58	0.19	0.04	132	62.40	0.34	4.34	0.07	0	0
	2.30	7.99	0.19	0.06	120	54.00	0.04	4.16	0.07	6.44	0.11

(a)

(b)

Figure 4.9 Cell morphology *A. terreus* during the production phase. The bioreactor was controlled at 30 °C, pH 2.0, 100 rpm with (a) 10 %DO and (b) 20 %DO. The C/N ratio of the production medium was 100/2.36.

For the pH, it was claimed that pH control also influenced itaconic acid production by facilitating the transport of itaconic acid across the membrane (Hevekerl et al., 2014b; Riscaldati et al., 2000). Failure to control the pH at the optimal condition resulted in the decreasing itaconic acid production (Table 2). It was reported that the pH higher than 5 or lower than 2 exhibited the negative effect on cell growth (Klement and Buchs, 2013). During the fermentation with the initial pH of 3.40, when the pH was left uncontrolled and dropped down to 1.85, itaconic acid production was stopped due to the severe stress on the fungal mycelia (Krull et al., 2017). Therefore, maintaining the pH at the optimal condition could control proper cell growth, itaconic acid production, and product transport across the membrane.

From all DO levels and pH studied, it was found that low DO level of 10 % and the pH of 2.00 gave the highest itaconic acid production. At this condition, it was found that the final itaconic acid titer at 10 %DO (35.65 g/L) was almost 3 times higher than that obtained from the fermentation with 20 %DO (12.19 g/L) (Table 4.4).

4.2.3 Correlation between morphology and itaconic acid production

The morphology of *A. terreus* during the production phase can be divided into 4 stages. Fig. 4.10 displays the morphological change along the fermentation at 10 % DO, pH 2.00. At 48 h when the production phase started, the morphology appeared to be pelletized (Figure 4.10(a), 4.10(e)). As the fermentation proceeded, the pellets became denser and the mycelial tips were elongated at 60 h (Figure 4.10(b)). During this stage, the fermentation broth became viscous (Figure 4.10(f)). Later at 84 h, the elongated tips were broken resulted in the freely dispersed mycelia in the fermentation

broth (Figure 4.10(c), 4.10(g)). During the last stage (108 h), the pellets were loosened and the freely dispersed mycelia were aggregated into clumps (Figure 4.10(d), 4.10(h)) accompanying with itaconic acid production (Figure 4.10(i)).

While in this study, when correlating the morphological change with the fermentation kinetics, it was revealed that the correct morphological form for itaconic acid production appeared to be the mycelial clumps (Figure 4.10). From the findings mentioned above, it is necessary to determine the suitable agitation and aeration rates to limit the shear stress affecting the change in morphology and to provide sufficient oxygen transfer during itaconic acid production (El-Imam and Du, 2014).

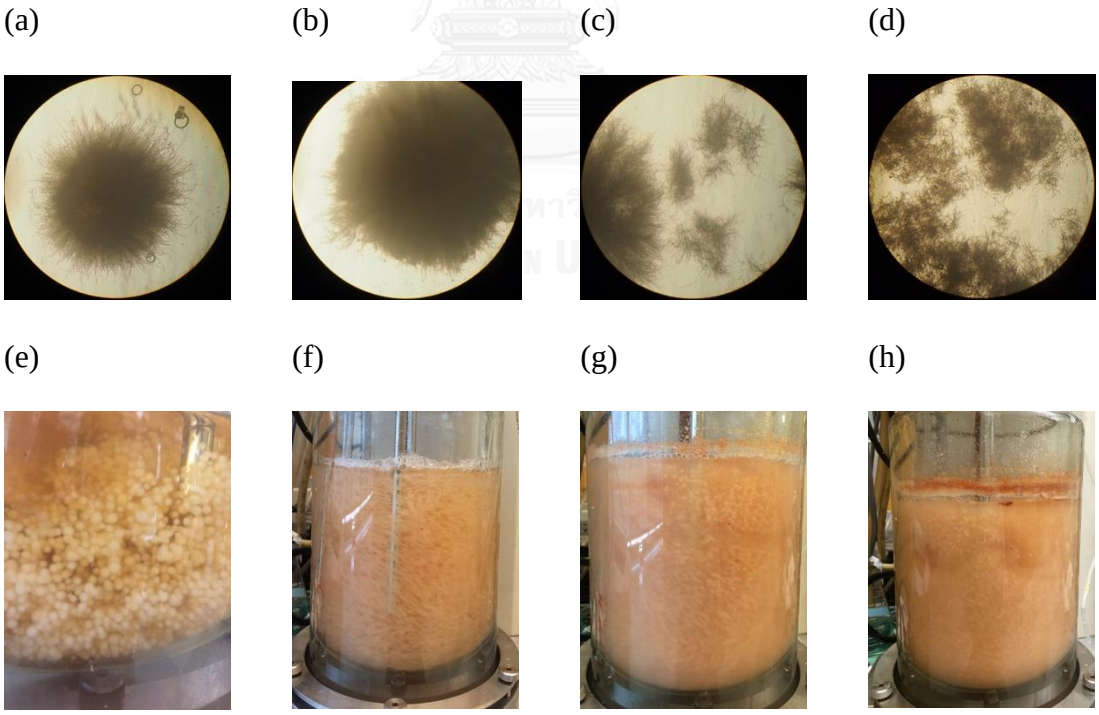

(i)

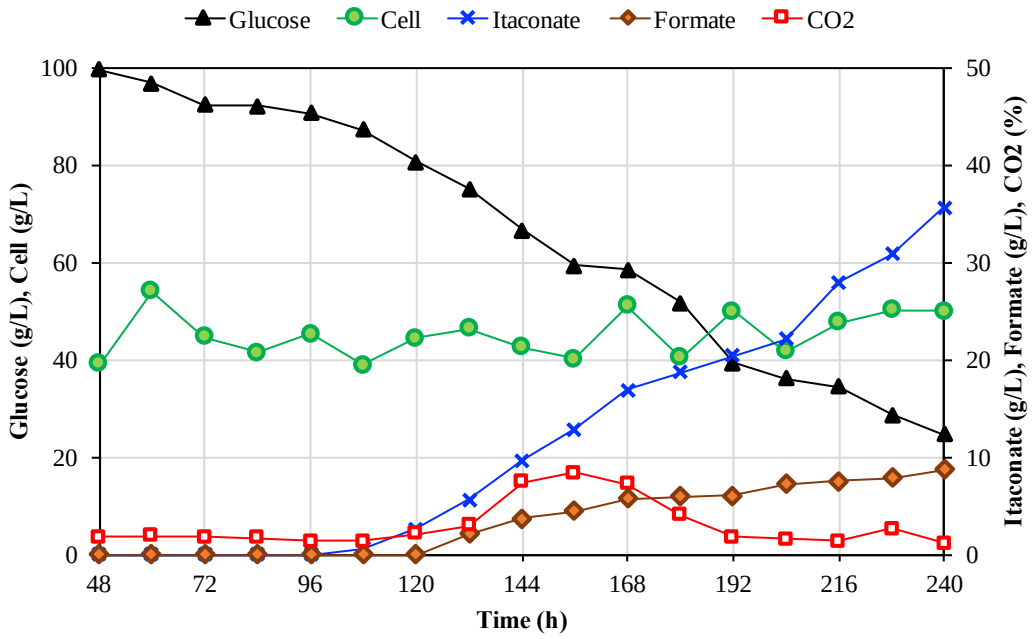

Figure 4.10 Morphological change during the production phase. The fermentation was controlled at 30 °C, 100 rpm, 10 %DO, pH 2.00. The C/N ratio of the medium was 100/2.36. (a) the pellets at 48 h, (b) the elongated tips at 60 h, (c) the freely dispersed mycelia at 84 h, (d) the mycelial clumps at 108 h, (e) the pelletized morphology at 48 h, (f) the dense pellets at 60 h, (g) the viscous broth at 84 h, (h) the clumps appeared all the bioreactor, (i) the kinetics profiles.

Furthermore, from figure 4.10(i), it was clear that cell biomass rather remained constant throughout this phase while itaconic acid started to produce at 96 h. This phenomenon could be explained by the oxidative phosphorylation being uncoupled from the glycolysis under low ammonium concentration and DO level. The glycolytic flux was rapidly enhanced for ATP regeneration via the substrate level phosphorylation under this condition (Snoek and Steensma 2007). As a result, pyruvate flux was shifted

towards itaconic acid production route instead of completing the oxidative TCA cycle for biosynthesis. By this technique, the metabolic flux would be better controlled during the production under the optimized conditions. From those mentioned above, it can be summarized that itaconic acid was produced under limited growth and the correct morphology. Therefore, non-growth associated product kinetics model can be applied for itaconic acid production in 2-phase fermentation by *A. terreus*.

Nonetheless, not only itaconic acid and cell biomass were generated during the production phase, major byproduct formate was formed in all conditions studied. From the kinetics profiles (data not shown), ethanol was observed later almost at the end of the fermentation in some conditions (Table 4.4). This indicated the change in metabolic fluxes that shifted towards the end products as the consequence of the controlled conditions. More formate was found at low DO level while pH seemed not affect formate formation. Therefore, one needs to further investigate the gene expression of the key enzymes responsible for this evidence.

4.2.4 Gene expression of the key enzymes responsible for itaconic acid production

Although a high final concentration with a high yield of itaconic acid was obtained via the 2-phase fermentation process proposed in this study, evidence of formate formation during the fermentation remained unclear. In contrast, in the typical 1-phase fermentation, most of the byproducts appeared to be the metabolites in the TCA cycle such as 2-oxoglutarate, one of the intermediates in the oxidation of succinate to fumarate under high DO level (Krull et al., 2017).

To better understand the biosynthesis of itaconic acid in *A. terreus* and thus to further improve the production performance, we observed the gene expression during the production phase and attempted to correlate the process conditions to the regulation of the genes of interest. Itaconic acid was produced via glycolysis and a part of TCA cycle (Figure 4.3). Glucose was converted to the key intermediate pyruvate. The key responsible enzyme in this route was phosphofructokinase. Pyruvate was converted to acetyl CoA by pyruvate dehydrogenase complex or being carboxylated to oxaloacetate by pyruvate carboxylase. The formation of itaconic acid involved the shuttle of intermediate metabolites between cytosol and mitochondria and utilized the different enzymes present in both cell compartments. Cis-aconitate was transported into the cytosol in exchange with malate via the mitochondrial TCA transporter. Cis-aconitate was then converted to itaconic acid by cis-aconitate decarboxylase. Later itaconic acid was secreted from the cytosol across the membrane via the major facilitator superfamily transporter.

Figure 4.11 describes the transcription levels of the genes encoding the key enzymes involved in the biosynthesis of itaconic acid during the production phase where the fermentation was controlled at 30 °C, 100 rpm, 10 %DO, pH 2.00. The expression of phosphofructokinase genes (*pfk*) in glycolysis was slightly changed during the production phase (Figure 4.11(a)) while other genes were noticeably changed either being up regulated or down regulated (Figures 4.11(b)-(e)). The evidence of down regulation of pyruvate dehydrogenase genes (*pdh*B, *pdh*C, *pdh*A and *pdh*X) with the up regulation of pyruvate carboxylase gene (*pyc*) from the heat map indicated that the pyruvate flux was shifted towards carboxylation to oxaloacetate as

the fermentation proceeded (Figures 4.11(a), 4.11(b), and 4.12). It was suggested that the limited nitrogen was responsible for this metabolic flux shift.

The fluctuation of the gene expression involved in the isomerization of citrate (citrate to cis-aconitate to isocitrate) could be explained by the down regulation of *pdh* genes and the up regulation of *pyc* (fold change more than 2) (Figures 4.11(c), 4.12). The up regulation of *pyc* resulted in the large pool of oxaloacetate in the cytosol. This induced the conversion of oxaloacetate to malate to be transported into the mitochondria while cis-aconitate was transported out at the mitochondrial TCA transporter. This phenomenon was confirmed by the up regulation of mitochondrial TCA transporter (*mttA*) and cis-aconitate decarboxylase (*cadA*) genes along with major facilitator superfamily transporter gene (*mfsA*) responsible for secreting itaconic acid to the fermentation broth (Figure 4.11(d)). Malate being transferred into the mitochondria was intended to be converted to oxaloacetate generating a large pool of oxaloacetate. To maintain the metabolic activity and balance the metabolic fluxes, more acetyl CoA was required so that citrate synthesis could be proceeded. To get more acetyl CoA, it was suggested that pyruvate was reacted with coenzyme A by pyruvate-formate lyase to form formate and acetyl CoA (Figure 4.11(d)). The evidence of formate formation during itaconic acid fermentation supported this hypothesis (Table 4.4). Although no annotated gene encoding pyruvate-formate lyase (*pfl*) was reported in *A. terreus*, the expression of formate dehydrogenase gene observed in this study as well as the CO_2 level in the fermentation broth (Figure 4.10(i)) confirmed our hypothesis.

Moreover, it was observed that the expression of the putative genes of succinate dehydrogenase, succinate coenzyme Q reductase, and the respiratory complex II that

catalyzed the oxidation of succinate to fumarate in the oxidative TCA cycle by simultaneously reducing ubiquinone to ubiquinol in the electron transport chain were low (Fig. 4.11(e)). Low dissolved oxygen was claimed to be responsible for the down regulation of these genes.

Therefore, the propose metabolic pathway of *A. terreus* indicating key genes responsible for itaconic acid synthesis could be summed up in figure 4.13. Since the metabolic flux towards itaconic acid production under low DO level where oxidative TCA cycle was incomplete, acetyl CoA could be obtained from an alternate route by pyruvate-formate lyase catalyzing pyruvate and coenzyme A in the mitochondria to acetyl CoA and formate (Stairs et al., 2011). As a result, the malate pool in the cytosol could be transported into the mitochondria to subsequently convert to oxaloacetate. On the other hand, itaconic acid was transported into the cytosol in exchange with malate. This eventually allowed the conversion of oxaloacetate and acetyl CoA to citrate isomers (citrate, cis-aconitate, and isocitrate), another key intermediate in itaconic acid production generating the metabolic flux balance. Stairs et al. (2011) claimed that pyruvate-formate lyase was the oxygen sensitive enzyme activated by *pfl* gene (Stairs et al., 2011). The literature survey of the eukaryotic genomic data by Stairs et al. (2011) revealed the diversity of microbial eukaryotic lineages that possessed *pfl* homologues and their activated enzymes. It was reported that many aerobic eukaryotes that experienced the low oxygen level turned on this alternated pathway for regenerating of coenzyme A (Stairs et al., 2011).

In contrast, pyruvate dehydrogenase complex was activated at a high DO level. Under this condition, the oxidative decarboxylation of pyruvate occurred and acetyl CoA was obtained. Acetyl CoA entered the TCA cycle regenerating the reducing

equivalents while ATP was generated in the coupled electron transport chain via the oxidative phosphorylation (Hartman et al., 2014; Patel et al., 2014; Stairs et al., 2011). This would by uncertain means result in a reduced malate pool in the cytosol. To enhance itaconic acid production, overexpression of *pyc* gene for pyruvate carboxylase activity in the cytosol was required in the fermentation under high DO level. By this method, the pyruvate pool could be balanced for malate production in the cytosol and acetyl CoA synthesis in the mitochondria for citrate isomer synthesis.

(a)

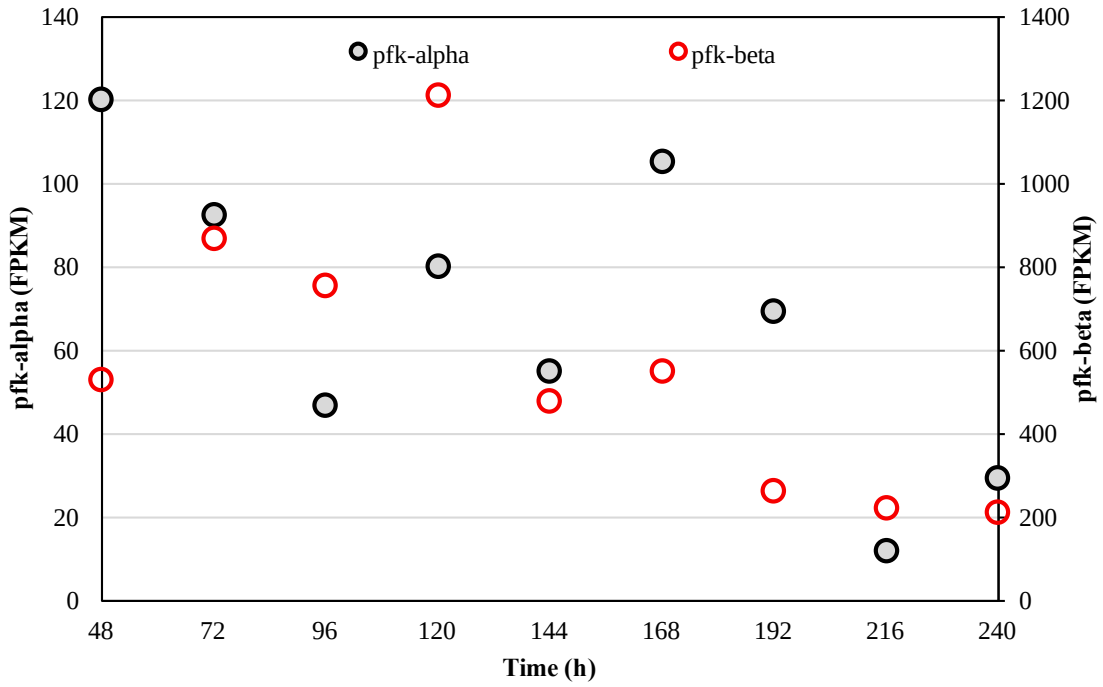
pfk-alpha
pfk-beta
pfk-alpha (FPKM)
pfk-beta (FPKM)
Time (h)
0
20
40
60
80
100
120
140
0
200
400
600
800
1000
1200
1400
48
72
96
120
144
168
192
216
240

(b)

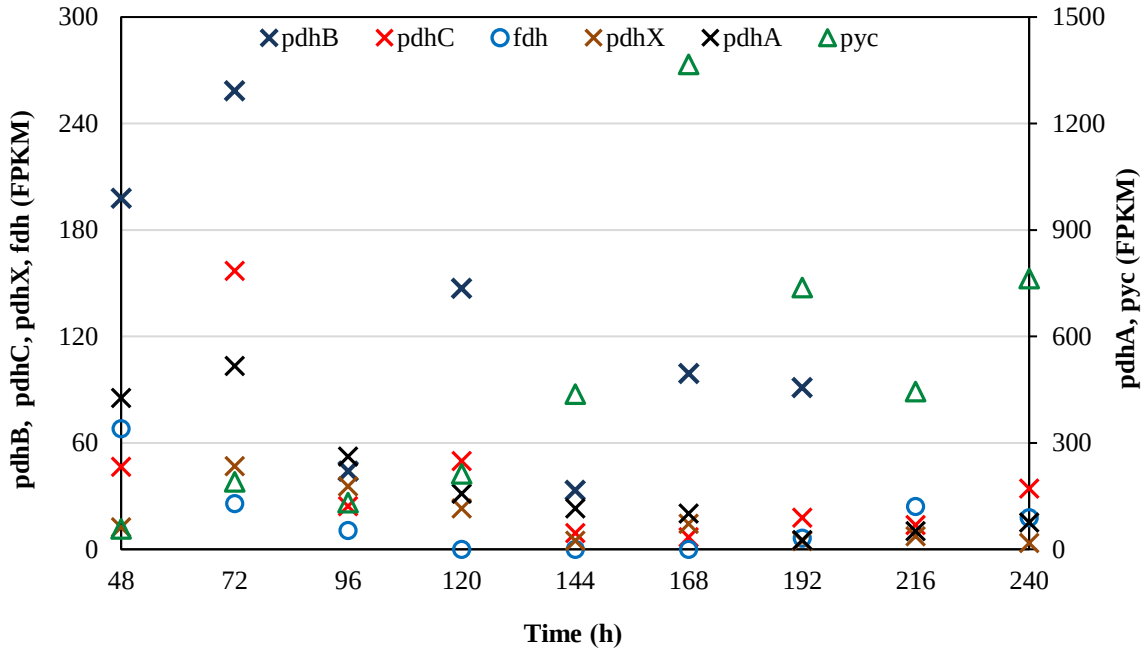
pdhB
pdhC
fdh
pdhX
pdhA
pyc
pdhB, pdhC, pdhX, fdh (FPKM)
pdhA, pyc (FPKM)
Time (h)
0
60
120
180
240
300
0
300
600
900
1200
1500
48
72
96
120
144
168
192
216
240

(c)

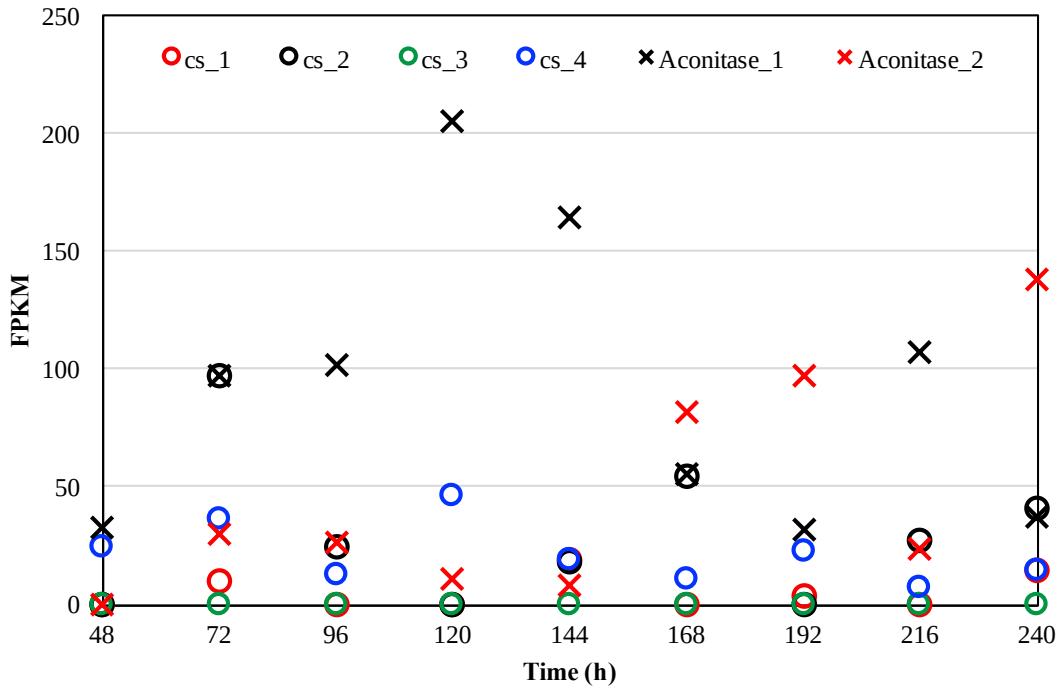
cs_1
cs_2
cs_3
cs_4
Aconitase_1
Aconitase_2
FPKM
250
200
150
100
50
0
48
72
96
120
144
168
192
216
240
Time (h)

(d)

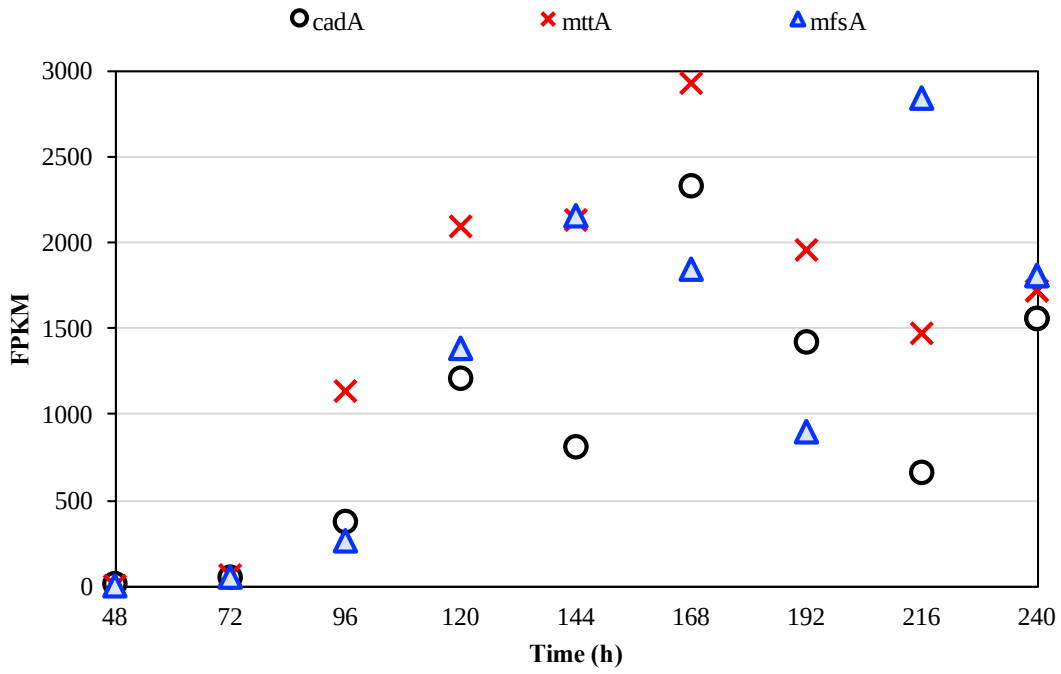
cadA
mttA
mfsA
FPKM
3000
2500
2000
1500
1000
500
0
48
72
96
120
144
168
192
216
240
Time (h)

(e)

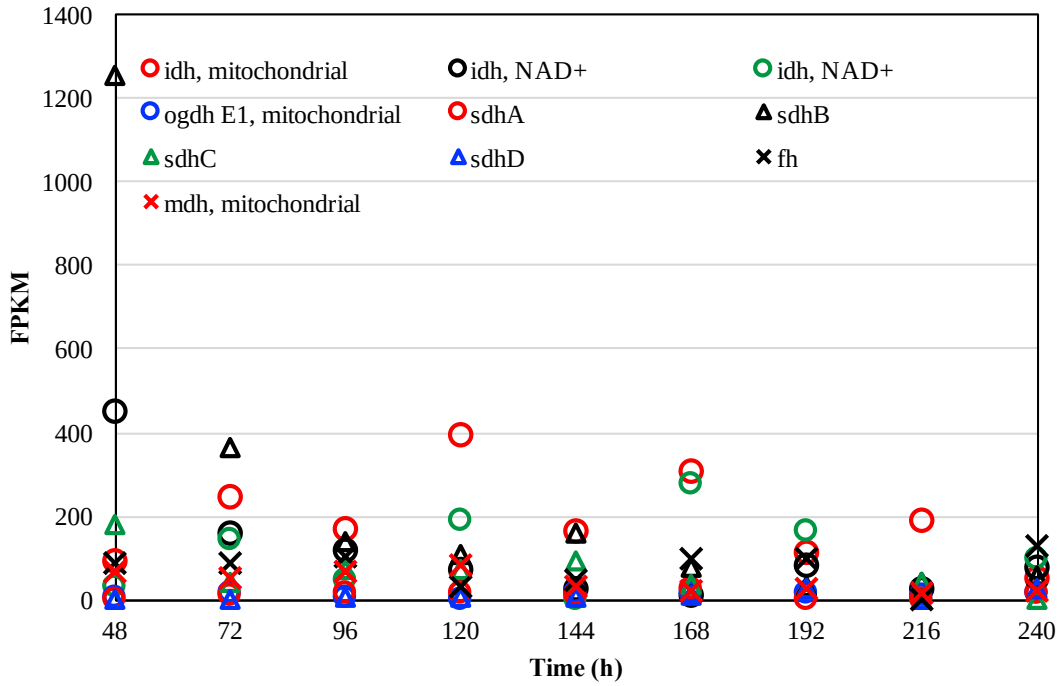

Figure 4.11 The transcription levels of cluster genes responsible for itoconate synthesis during the production phase of *A. terreus* cultivated at 30 °C, 100 rpm, 10 %DO, pH 2.00. The C/N ratio of the medium was 100/2.36. (a) glycolytic genes, (b) at pyruvate nodes, (c) citrate synthesis/isomerization, (d) itaconic acid synthesis, and (e) mitochondrial OGDH and MDH clusters.

gene_id	Gene Name	log2(fold_change)						
		48 vs. 72	48 vs. 96	48 vs. 120	48 vs. 144	48 vs. 168	48 vs. 192	48 vs. 240
ATEG_07332	ATEG_07332, alpha-pfk	0.88	0.67	1.51	0.03	0.24	-0.89	-1.26
ATEG_07646	ATEG_07646, beta-pfk	-0.21	-1.19	-0.26	-0.95	0.00	-0.68	-3.35
ATEG_03737	ATEG_03737, pdhB	0.55	-2.00	-0.11	-2.39	-0.81	-1.00	-2.98
ATEG_04262	ATEG_04262, pdhC	1.92	-0.78	0.42	-2.17	-2.58	-1.26	-1.76
ATEG_06361	ATEG_04262, pdhA	0.44	-0.54	-1.12	-1.71	-1.89	-3.89	-3.06
ATEG_01642	ATEG_01642, pdhX	2.09	1.68	1.22	-1.17	0.42	-1.26	-0.76
ATEG_05433	ATEG_05433, pyc	1.89	1.35	2.21	3.10	4.76	3.79	2.94

Figure 4.12 Heat map summarizing the differential expression of the glycolytic genes responsible for itaconic acid production in *A. terreus* during the production phase. The number in the box indicates the differential gene expression level compared with that at the starting time (48 h). The green box represents the up regulation of the gene. The red box represents the down regulation of the gene. The black box indicates the slightly change in gene expression level (log2(fold_change)) less than 2).

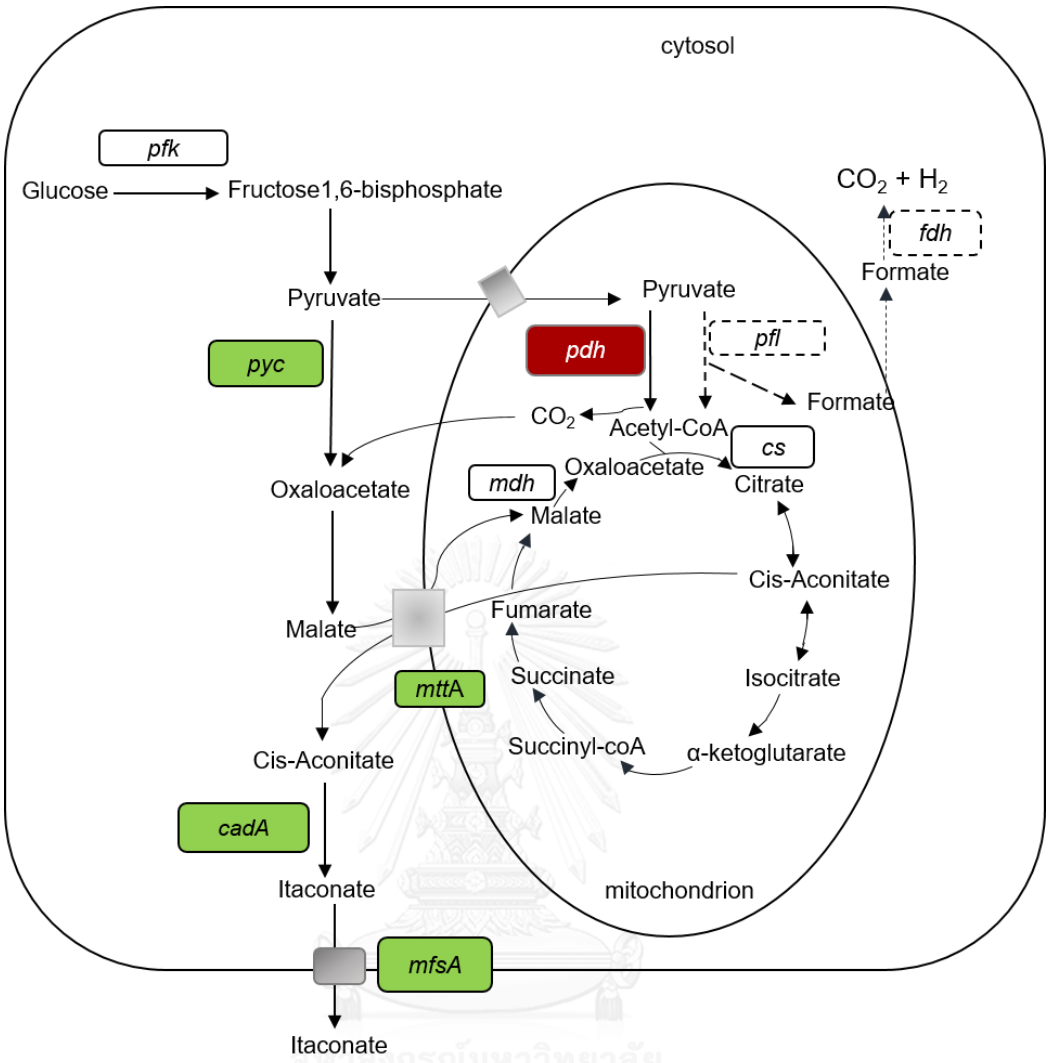

Figure 4.13 Proposed metabolic pathway of *A. terreus* indicating key genes responsible for itaconic acid synthesis.

CHAPTER 5

CONCLUSIONS AND RECOMMENDATIONS

5.1 Conclusions

The biosynthesis of itaconic acid by *Aspergillus terreus* involved both biosynthesis and transport of metabolites across the cell compartments. In a previous study, it was claimed that itaconic acid production was usually associated with the biomass production. Therefore, balancing the metabolic flux towards itaconic acid production to achieve high production yield was complicated. As a result, the typical itaconic acid fermentation suffered from low final product yield and productivity. To better understand the root causes mentioned above and to propose alternative technique to enhance itaconic acid production, two approaches were employed in this study.

In the first approach, the activity of pyruvate carboxylase (PC) was manipulated by the presence of L-aspartate in order to regulate ATP regeneration during itaconic acid production. The presence of L-aspartate at 10 mM in the production medium directly repressed the activity of PC in the living culture of *A. terreus* because of the limited malate flux in the cytosol to be transported across the malate/cis-aconitate antiporter. This resulted in a large pool of pyruvate flux shuffling into the mitochondrion compartment. To maintain the metabolic flux balance under limited nitrogen, *A. terreus* stimulated the conversion of the large pool of cis-aconitate into

itaconic acid by transporting cis-aconitate in exchange with malate at the antiporter for conversion to itaconic acid by cis-aconitate decarboxylase. This phenomenon was clearly described by the increasing activity of cis-aconitate decarboxylase. This subsequently resulted in the improved final concentration and yield of itaconic acid by 60.32 % and 8.33 %, respectively compared to those obtained from the control fermentation. By this, the lag phase during the production phase was also shortened which gave the improved overall productivity.

In the second approach, the 2-phase fermentation process was employed in itaconic acid production for better control of metabolic flux towards itaconic acid production route. Unlike the typical 1-phase fermentation, itaconic acid production in the 2-phase fermentation approach followed non-growth associated product formation kinetics model where itaconic acid production was not associated with the cell growth. This was confirmed by the presence of itaconic acid in the fermentation broth when ammonium and phosphate became limited. Contrary to those claimed in 1-phase fermentation, by the 2-phase fermentation, low DO level enhanced itaconic acid production because it promoted the correct morphology in the form of mycelial clumps. In addition, with low DO level, glycolysis was uncoupled with oxidative phosphorylation and stimulated substrate level phosphorylation for ATP regeneration. As a result, this drove the increase in glycolytic flux for the key intermediate, pyruvate. With the low DO level, this resulted in the down regulation of the genes in pyruvate dehydrogenase complex as the TCA was shunted. To maintain the balance of metabolic flux under the low DO level and the limited ammonium and phosphate, *A. terreus* turned on the alternated metabolic route. As a result, the available pyruvate was then reacted with coenzyme A by pyruvate-formate lyase resulting in formate and acetyl

CoA ready for shuttling towards cis-aconitate. Cis-aconitate was then transported across the malate/cis-aconitate antiporter for synthesis of itaconic acid by cis-aconitate decarboxylase. The results in this study also suggested that pH was responsible for transporting of metabolites and itaconic acid across the cell compartments to allow biosynthesis and maintain the balance of metabolic fluxes. Thus, itaconic acid production by this approach could reach 72 % of the theoretical yield (0.72 g/g) with the highest yield and titer of 0.52 g/g and 35.65 g/L, respectively in the fermentation at low DO level of 10 %, pH of 2.0 and the C/N ratio of 100:2.36.

From the findings addressed in this study, it is clear that the production of itaconic acid by *A. terreus* involves several biosynthetic reactions and metabolite transport across the cell compartments. Thus, to facilitate the production, it is mandatory to control both phenomena at the suitable rates.

5.2 Recommendations

The better understanding on the enzymes and genes regulation in itaconic acid fermentation was acquired in this study. The information suggested that pyruvate metabolism into oxaloacetate in cytosol and acetyl-CoA in mitochondria should be balanced for approaching the reaction equilibrium towards itaconic acid production. This was claimed as the key success factor in improved production performance. Hence, developing the new approach to serve on this purpose is challenging.

From the morphological study obtained, it was suggested that the correct morphological structure for itaconic acid production by *A. terreus* was in the form of clumps. Low DO level helped maintain this structure during itaconic acid production. Nevertheless, during the 2-phase fermentation, it took a long time to reach the correct morphological stage. This subsequently resulted in the low reactor productivity. In order to shorten this stage, the knowledge on morphological structure should be further examined.

REFERENCES

Acar, S., M. Yucel, and H. Hamamci. 2007. Purification and characterisation of two isozymes of pyruvate decarboxylase from *Rhizopus oryzae*. *Enzyme and Microbial Technology*. 40:675-682.

Adina-Zada, A., T.N. Zeczycki, and P.V. Attwood. 2012. Regulation of the structure and activity of pyruvate carboxylase by acetyl CoA. *Archives of Biochemistry and Biophysics.* 519:118-130.

Baykov, A.A., O.A. Evtushenko, and S.M. Avaeva. 1988. A malachite green procedure for orthophosphate determination and its use in alkaline phosphatase-based enzyme immunoassay. *Analytical Biochemistry.* 171:266-270.

Bentley, R., and C.P. Thiessen. 1957. Biosynthesis of itaconic acid in *Aspergillus terreus*. III. The properties and reaction mechanism of cis-aconitic acid decarboxylase. *Journal of Biological Chemistry*. 226:703-720.

Berg, J.M., J.L. Tymoczko, and L. Stryer. 2002. Entry to the citric acid cycle and metabolism through it are controlled. *In* Biochemistry. W.H. Freeman, editor, New York.

Boer, V.M., C.A. Crutchfield, P.H. Bradley, D. Botstein, and J.D. Rabinowitz. 2010. Growth-limiting intracellular metabolites in yeast growing under diverse nutrient limitations. *Molecular Biology of the Cell.* 21:198-211.

Bonnarme, P., B. Gillet, A.M. Sepulchre, C. Role, J.C. Beloeil, and C.Ducrocq. 1995. Itaconate biosynthesis in *Aspergillus terreus*. *Journal of Bacteriology*. 177.

Calam, C.T., A.E. Oxford, and H. Raistrick. 1939. Studies in the biochemistry of micro-organisms: itaconic acid, a metabolic product of a strain of *Aspergillus terreus* Thom. *Biochemical Journal*. 33:1488–1495.

Capuder, M., T. Solar, M. Bencina, and M. Legisa. 2009. Highly active, citrate inhibition resistant form of *Aspergillus niger* 6-phosphofructo-1-kinase encoded by a modified *pfkA* gene. *Journal of Biotechnology*. 144:51-57.

Choi, S., C.W. Song, J.H. Shin, and S.Y. Lee. 2015. Biorefineries for the production of top building block chemicals and their derivatives. *Metabolic Engineering*. 28:223-239.

Deak, E., S.D. Wilson, E. White, J.H. Carr, and S.A. Balajee. 2009. *Aspergillus terreus* accessory conidia are unique in surface architecture, cell wall composition and germination kinetics. *PLoS One*. 4:e7673.

Dwiarti, L., M. Otsuka, S. Miura, M. Yaguchi, and M. Okabe. 2007. Itaconic acid production using sago starch hydrolysate by *Aspergillus terreus* TN484-M1. *Bioresource Technology*. 98:3329-3337.

Dwiarti, L., K. Yamane, H. Yamatani, P. Kahar, and O. M. 2002. Purification and characterization of cis-aconitic acid decarboxylase from *Aspergillus terreus* TN484-M1. *Journal of Bioscience and Bioengineering*. 94:29-33.

El-Imam, A.A., and C. Du. 2014. Fermentative Itaconic Acid Production. *Journal of Biodiversity, Bioprospecting and Development*. 1:119.

Gao, Q., J. Liu, and L. Liu. 2014. Relationship between morphology and itaconic acid production by *Aspergillus terreus*. *Journal of Microbiology and Biotechnology*. 24:168-176.

Guevarra, E.D., and T. Tabuchi. 1990. Accumulation of itaconic, 2-hydroxyparaconic, itatartaric, and malic acids by strains of of the Genus *Ustilago*. *Agricultural and Biological Chemistry*. 54:2353-2358.

Gyamerah, M.H. 1995. Oxygen requirement and energy relations of itaconic acid fermentation by *Aspergillus terreus* NRRL 1960. *Applied Microbiology and Biotechnology*. 44:20-26.

Habison, A., C.P. Kubicek, and M. Röhr. 1983. Partial purification and regulatory properties of phosphofructokinase from *Aspergillus niger*. *Biochemical Journal*. 209:669-676.

Hartman, T., B. Weinrick, C. Vilcheze, M. Berney, J. Tufariello, G.M. Cook, and W.R. Jacobs, Jr. 2014. Succinate dehydrogenase is the regulator of respiration in *Mycobacterium tuberculosis*. *PLoS Pathogens*. 10:e1004510.

Haskins, R.H., J.A. Thorn, and B. Boothroyd. 1955. Biochemistry of the Ustilaginales: XI. Metabolic products of *Ustilago zeae* in submerged culture. *Canadian Journal of Microbiology*. 1:749-756.

Hevekerl, A., A. Kuenz, and K.D. Vorlop. 2014a. Filamentous fungi in microtiter plates-an easy way to optimize itaconic acid production with *Aspergillus terreus*. *Applied Microbiology and Biotechnology*. 98:6983-6989.

Hevekerl, A., A. Kuenz, and K.D. Vorlop. 2014b. Influence of the pH on the itaconic acid production with *Aspergillus terreus*. *Applied Microbiology and Biotechnology*. 98:10005-10012.

Holness, M.J., and M.C. Sugden. 2003. Regulation of pyruvate dehydrogenase complex activity by reversible phosphorylation. *Biochemical Society Transactions* 31:1143-1151.

Hossain, M., J.D. BrooksI, and S. Maddox. 1984. The effect of the sugar source on citric acid production by *Aspergillus niger*. *Applied Microbiology and Biotechnology*. 19:393–397.

Huang, X., X. Lu, Y. Li, X. Li, and L.J. J. 2014. Improving itaconic acid production through genetic engineering of an industrial *Aspergillus terreus* strain. *Microbial Cell Factories*. 13:1-9.

Jaklitsch, W.M., C.P. Kubicek, and M.C. Scrutton. 1991. The subcellular organization of itaconate biosynthesis by *Aspergillus terreus*. *Journal of General Microbiology* 137:533-539. .

Kanamasa, S., L. Dwiarti, M. Okabe, and E.Y. Park. 2008. Cloning and functional characterization of the cis-aconitic acid decarboxylase (CAD) gene from *Aspergillus terreus*. *Applied Microbiology and Biotechnology*. 80:223-229.

Kautola, H., M. Vahvaselka, Y.Y. Linko, and P. Linko. 1985. Itaconic acid production by immobilized *Aspergillus terreus* from xylose and glucose. *Biotechnology Letters* 7:167-172.

Klement, T., and J. Buchs. 2013. Itaconic acid-a biotechnological process in change. *Bioresource Technology*. 135:422-431.

Krull, S., A. Hevekerl, A. Kuenz, and U. Prusse. 2017. Process development of itaconic acid production by a natural wild type strain of *Aspergillus terreus* to reach industrially relevant final titers. *Applied Microbiology and Biotechnology*. 101:4063-4072.

Kubicek, C.P., and M. Rohr. 1985. Aconitase and citric acid fermentation by *Aspergillus niger*. *Applied and Environmental Microbiology*. 50:1336-1338.

Kuenz, A., Y. Gallenmuller, T. Willke, and K.D. Vorlop. 2012. Microbial production of itaconic acid: developing a stable platform for high product concentrations. *Applied Microbiology and Biotechnology*. 96:1209-1216.

Levinson, W.E., C.P. Kurtzman, and T.M. Kuo. 2006. Production of itaconic acid by *Pseudozyma antarctica* NRRL Y-7808 under nitrogen-limited growth conditions. *Enzyme and Microbial Technology*. 39:824-827.

Li, A., N. van Luijk, M. ter Beek, M. Caspers, P. Punt, and M. van der Werf. 2011. A clone-based transcriptomics approach for the identification of genes relevant for itaconic acid production in *Aspergillus*. *Fungal Genetics and Biology*. 48:602-611.

Lowry, O.H., N.J. Rosebrough, A.L. Farr, and R.J. Randall. 1951. Protein measurement with the Folin phenol reagent. *Journal of Biological Chemistry.* 193:265-275.

Myers, D.E., B. Tolbert, and M.F. Utter. 1983. Activation of yeast pyruvate carboxylase: interactions between acyl coenzyme A compounds, aspartate, and substrates of the reaction. *Biochemistry*. 22:5090-5096.

Okabe, M., D. Lies, S. Kanamasa, and E.Y. Park. 2009. Biotechnological production of itaconic acid and its biosynthesis in *Aspergillus terreus*. *Applied Microbiology and Biotechnology*. 84:597-606.

Osmani, S.A., F.A. Marston, I.P. Selmes, A.G. Chapman, and M.C. Scrutton. 1981. Pyruvate carboxylase from *Aspergillus nidulans*. Regulatory properties. *European Journal of Biochemistry*. 118:271-278.

Osmani, S.A., F.A. Marston, I.P. Selmes, A.G. Chapman, and M.C. Scrutton. 1985. Pyruvate carboxylase from *Aspergillus nidulans*. Regulatory properties. *European Journal of Biochemistry*. 118:271–278.

Osmani, S.A., and M.C. Scrutton. 1984. The sub-cellular localisation and regulatory properties of pyruvate carboxylase from *Rhizopus arrhizus*. *European Journal of Biochemistry*. 147:119–128.

Papagianni, M. 2007. Advances in citric acid fermentation by *Aspergillus niger*: biochemical aspects, membrane transport and modeling. *Biotechnology Advances*. 25:244-263.

Papagianni, M., F. Wayman, and M. Mattey. 2005. Fate and role of ammonium ions during fermentation of citric acid by *Aspergillus niger*. *Applied and Environmental Microbiology*. 71:7178-7186.

Park, Y., M. Itida, N. Ohta, and M. Okabe. 1994. Itaconic acid production using an air-lift bioreactor in repeated batch culture of *Aspergillus terreus*. *Journal of Fermentation and Bioengineering.* 77:329-331.

Patel, K.P., T.W. O'Brien, S.H. Subramony, J. Shuster, and P.W. Stacpoole. 2012. The spectrum of pyruvate dehydrogenase complex deficiency: clinical, biochemical and genetic features in 371 patients. *Molecular Genetics and Metabolism*. 105:34-43.

Patel, M.S., N.S. Nemeria, W. Furey, and F. Jordan. 2014. The pyruvate dehydrogenase complexes: structure-based function and regulation. *Journal of Biological Chemistry*. 289:16615-16623.

Pfeifer, V.F., C. Vojnovich, and E.N. Heger. 1952. Itaconic acid by fermentation with *Aspergillus terreus*. *Journal of Industrial and Engineering Chemistry*. 44:2975–2980.

Riscaldati, E., M. Moresi, F. Federici, and M. Petruccioli. 2000. Effect of pH and stirring rate on itaconate production by *Aspergillus terreus*. *Journal of Biotechnology* 83: 219–230.

Saha, B.C. 2017. Emerging biotechnologies for production of itaconic acid and its applications as a platform chemical. *Journal of Industrial Microbiology and Biotechnology*. 44:303-315.

Schimmel, T.G. 1998. Effect of butyrolactone I on the producing fungus, *Aspergillus terreus*. *Applied and Environmental Microbiology*. 64:3707-3712

Songserm, P., S. Thitiprasert, V. Tolieng, J. Piluk, S. Tanasupawat, S. Assabumrungrat, S.T. Yang, A. Karnchanatat, and N. Thongchul. 2015. Regulating pyruvate carboxylase in the living culture of *Aspergillus terreus* Nrrl 1960 by L-Aspartate for enhanced itaconic acid production. *Applied biochemistry and biotechnology*. 177:595-609.

Stairs, C.W., A.J. Roger, and V. Hampl. 2011. Eukaryotic pyruvate formate lyase and its activating enzyme were acquired laterally from a Firmicute. *Molecular Biology and Evolution*. 28:2087-2099.

Steiger, M.G., M.L. Blumhoff, D. Mattanovich, and M. Sauer. 2013. Biochemistry of microbial itaconic acid production. *Frontiers in Microbiology*. 4:23.

Strelko, C.L., W. Lu, F.J. Dufort, T.N. Seyfried, T.C. Chiles, J.D. Rabinowitz, and M.F. Roberts. 2011. Itaconic acid is a mammalian metabolite induced during macrophage activation. *Journal of the American Chemical Society*. 133:16386-16389.

Tabuchi, T., T. Sugisawa, T. Ishidori, T. Nakahara, and J. Sugiyama. 1981. Itaconic acid fermentation by a yeast belonging to the Genus *Candida*. *Agricultural and Biological Chemistry*. 45:475-479.

Transparency market research. 2015. Itaconic Acid market is expected to reach US$ 204.6 Mn by 2023. In: Itaconic Acid market: global industry analysis, size, share, growth, trends and forecast 2015–2023. Vol. 26 Jul 2015.

Tevz, G., M. Bencina, and M. Legisa. 2010. Enhancing itaconic acid production by *Aspergillus terreus*. *Applied Microbiology and Biotechnology*. 87:1657-1664.

Thitiprasert, S., P. Songserm, W. Boonkong, S. Sooksai, K. Kodama, and N. Thongchul. 2014. Manipulating pyruvate decarboxylase by addition of enzyme regulators during fermentation of *Rhizopus oryzae* to enhance lactic acid production. *Applied biochemistry and biotechnology*. 174:1795-1809.

Tzollas, N.M., G.A. Zachariadis, A.N. Anthemidis, and J.A. Stratis. 2010. A new approach to indophenol blue method for determination of ammonium in geothermal waters with high mineral content. *International Journal of Environmental Analytical Chemistry*. 90:115-126.

Willke, T., and K.D. Vorlop. 2001. Biotechnological production of itaconic acid. *Applied Microbiology and Biotechnology*. 56:289-295.

Yahiro, K., S. Shibata, S.R. Jia, Y. Park, and M. Okabe. 1997. Efficient itaconic acid production from raw corn starch. *Journal of Fermentation and Bioengineering*. 84:375-377.

Yahiro, K., T. Takahama, Y. Park, and M. Okabe. 1995. Breeding of *Aspergillus terreus* mutant TN-484 for itaconic acid production with high yield. *Journal of Fermentation and Bioengineering*. 79:506-508.

Zeczycki, T.N., M.S. Maurice, and P.V. Attwood. 2010. Inhibitors of Pyruvate Carboxylase. *Open Enzyme Inhibition Journal*. 3:8-26.

Zhang, B., C.D. Skory, and S.T. Yang. 2012. Metabolic engineering of *Rhizopus oryzae*: effects of overexpressing pyc and pepc genes on fumaric acid biosynthesis from glucose. *Metabolic Engineering*. 14:512-520.

Zhou, J., L. Liu, Z. Shi, G. Du, and J. Chen. 2009. ATP in current biotechnology: regulation, applications and perspectives. *Biotechnology Advances*. 27:94-101.

APPENDIX A

Calibration curve for protein and enzyme activity determination

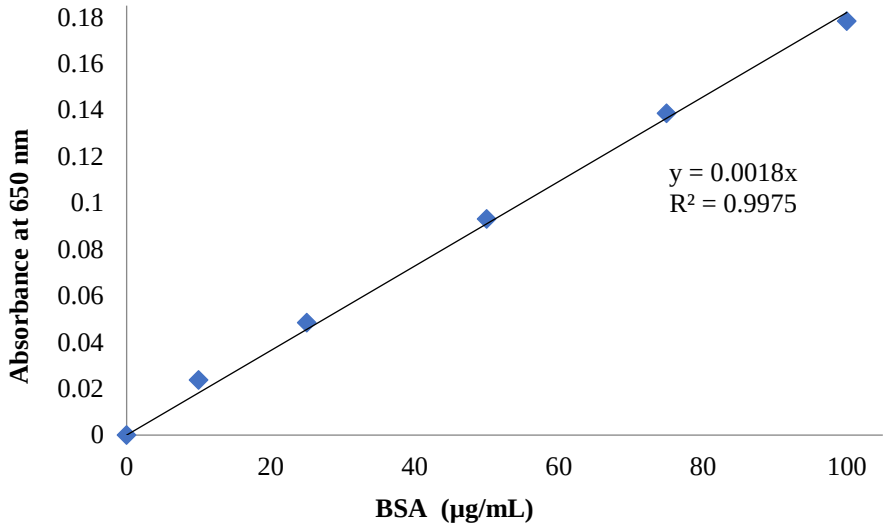

Figure A1 Standard of bovine serum albumin (BSA) for protein determination

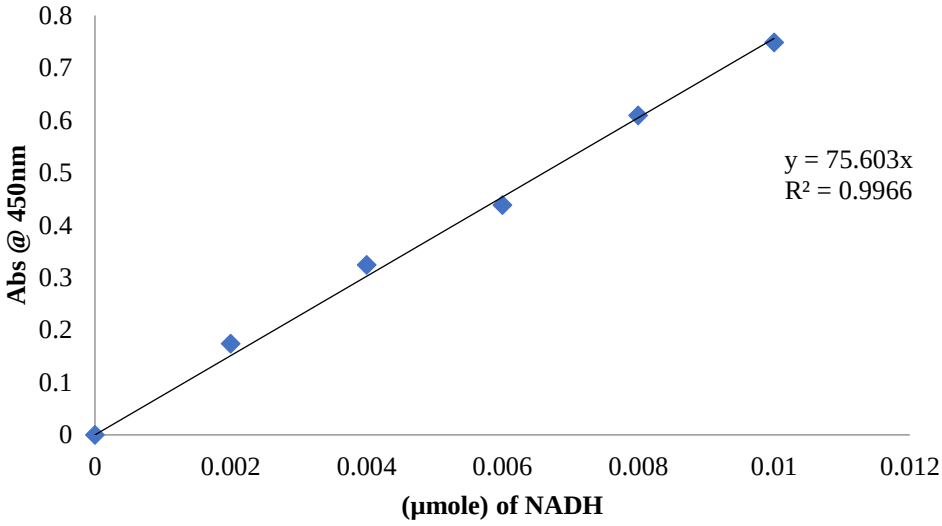

Figure A2 Standard of NADH for phosphofructokinase assay

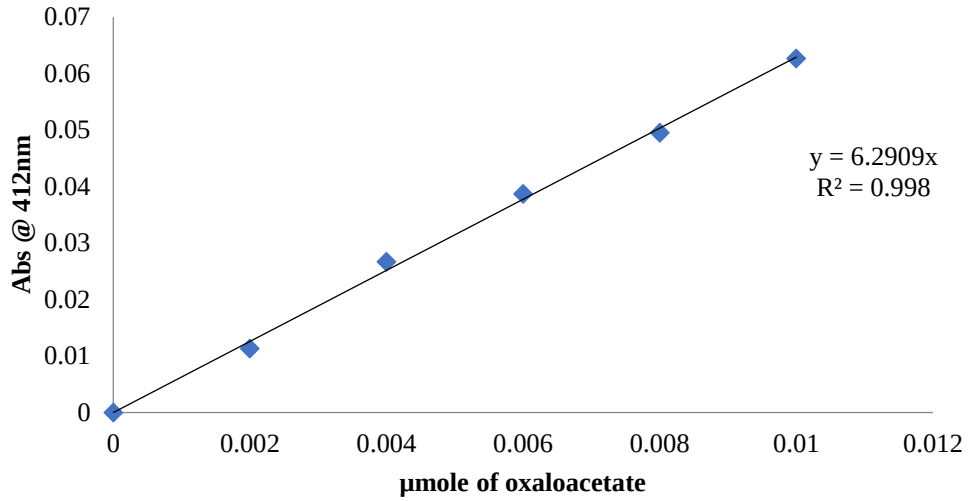

Figure A3 Standard of oxaloacetate for pyruvate carboxylase assay

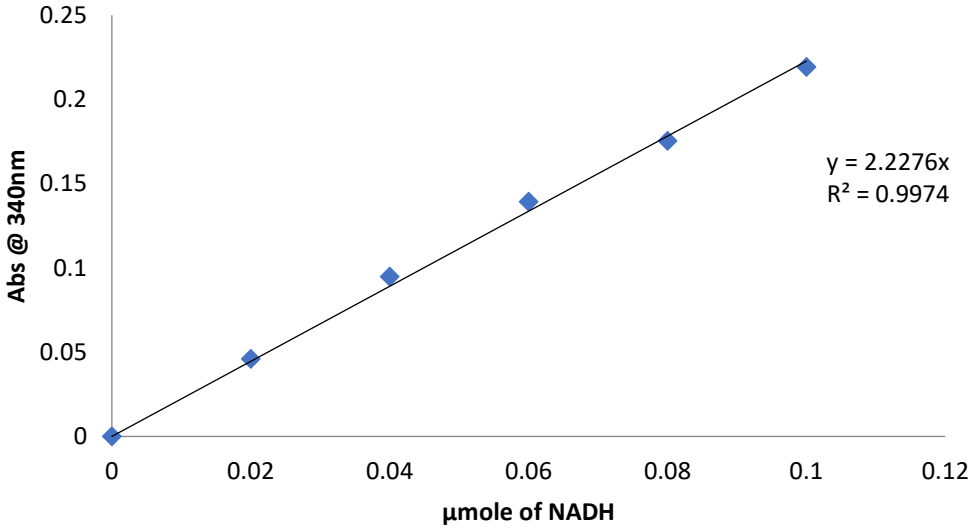

Figure A4 Standard of NADH for pyruvate dehydrogenase assay

APPENDIX B

Additional transcriptomic analysis results

Table A1 Transcription levels of the selected genes involved in itaconic acid synthesis during the production phase where the DO level was maintained at 10 %.

Gene id	Gene name	Fragments per kilo base per million reads (FPKM) at a certain time								
		48 h	72 h	96 h	120 h	144 h	168 h	192 h	216 h	240 h
Glycolysis										
ATEG_07646	6-phosphofructokinase beta subunit (pfk-beta)	530.72	869.52	754.93	1210.66	478.63	549.3	263.60	222.64	214.08
ATEG_07332	6-phosphofructokinase alpha subunit (pfk-alpha)	119.95	92.48	46.89	80.08	55.07	105.16	69.18	11.84	29.32
ATEG_03737	Pyruvate dehydrogenase (acetyltransferring) (PDH component E1-α) (pdhB)	197.87	258.55	44.20	147.21	33.37	99.13	91.3	25.11	87.07
ATEG_04262	Pyruvate dehydrogenase (acetyltransferring) (PDH component E1-β) (pdhC)	46.67	157.01	24.32	49.85	9.18	6.82	17.94	13.82	34.22
ATEG_06361	Dihydrolipoyllysine-residue acetyltransferase (Pyruvate dehydrogenase component E2) (pdhA)	427.17	517.08	261.754	157.25	115.86	101.21	26.63	51.28	76.20
ATEG_01642	Pyruvate dehydrogenase complex component X (E3-binding protein) (pdhX)	61.95	234.491	177.60	115.82	24.38	72.421	23.82	36.69	18.17
ATEG_05433	Pyruvate carboxylase (pyc)	57.67	190.30	131.80	213.26	437.34	1367.13	737.98	445.33	763.31

Citrate isomer production										
ATEG_07790	Citrate synthase (*cs*)	0.00	10.28	0.00	0.00	19.24	0.00	3.76	0.00	14.34
ATEG_07882	Citrate synthase (*cs*)	0.00	97.49	24.17	0.00	18.25	54.20	0.00	27.46	40.80
ATEG_05030	Citrate synthase (*cs*)	0.00	0.00	0.00	0.00	0.00	0.00	0.00	0.00	0.00
ATEG_07199	Citrate synthase (*cs*)	24.83	36.54	12.94	46.41	19.54	10.88	22.91	7.35	14.57
ATEG_02937	Aconitase	32.59	96.93	101.93	205.18	164.92	55.11	32.23	107.54	36.88
ATEG_03325	Aconitase	0.00	29.59	26.19	10.74	7.91	82.25	97.40	23.81	138.59
Itaconate cluster										
ATEG_09970	Mitochondrial TCA transporter (*mtt*A)	0.00	64.31	1131.69	2090.81	2130.19	2931.38	1961.36	1467.01	1722.42
ATEG_09971	Cis-aconitate decarboxylase (*cad*A)	11.30	49.90	379.88	1213.16	813.79	2328.12	1418.24	662.53	1556.35

ATEG_09972	Major facilitator superfamily transporter (mfsA)	0.00	53.81	266.76	1389.66	2156.86	1844.73	898.73	2841.68	1807.96
Oxidative TCA										
ATEG_01603	Isocitrate dehydrogenase, mitochondrial	95.82	249.35	168.56	393.46	162.63	309.79	116.07	191.53	52.71
ATEG_00467	Isocitrate dehydrogenase (NAD) subunit	450.58	161.07	117.42	72.20	26.60	13.17	83.16	26.68	79.31
ATEG_07408	Isocitrate dehydrogenase (NAD) subunit	30.04	142.12	46.97	192.53	0.00	276.52	166.32	0.00	99.13
ATEG_03911	2-oxoglutarate dehydrogenase E1 component, mitochondrial	4.85	15.30	7.58	0.00	14.31	14.88	17.90	12.92	19.21

ATEG_01694	Succinate dehydrogenase [uniquinone] flavoprotein subunit, mitochondrial	0.00	0.00	6.45	6.61	4.87	10.84	24.73	0.00	29.03
ATEG_07205	Fumarate hydratase class II	89.65	87.97	101.24	31.92	47.04	96.06	96.52	0.00	131.50
ATEG_05653	Malate dehydrogenase, mitochondrial	67.24	53.02	65.71	80.81	29.77	22.11	27.15	14.93	22.19
Major byproduct formate										
ATEG_05685	Formate dehydrogenase	68.06	25.76	10.64	0.00	0.00	0.00	6.28	24.18	17.97

VITA

Miss Pajareeya Songserm was born on Friday 4th October, 1985, in Udonthani, Thailand. In 2008, she graduated with a Bachelor's degree of Science in Microbiology, from Khonkaen University. Then, she graduated with a Master's degree of Science in Industrial Microbiology, from Chulalongkorn University. After that time, she has been studied for a doctoral degree in Biotechnology, Faculty of Science, Chulalongkorn University.

Research presentation experience

Pajareeya Songserm, Regulating Pyruvate Carboxylase in the Living Culture of Aspergillus Terreus NRRL1960 by L-Aspartate for Enhanced Itaconic Acid Production, 2015 AIChE Annual Meeting, Salt Lake City, The United State of America, November 11, 2015.

Pajareeya Songserm, Shang-Tian Yang, Aphichart Karnchanatat and Nuttha Thongchul, Manipulating pyruvate carboxylase in Aspergillus terreus NRRL 1960 with L-aspartate in the medium for improved itaconic acid production, RGJ-Ph.D. Congress 18, Nonthaburi, Thailand, June 8, 2017.

International Publication

Pajareeya Songserm, Sitanan Thitiprasert, Vasana Tolieng, Jiraporn Piluk, Somboon Tanasupawat, Sutthichai Assabumrungrat, Shang-Tian Yang, Aphichart Karnchanatat and Nuttha Thongchul. 2015. Regulating Pyruvate Carboxylase in the Living Culture of Aspergillus Terreus NRRL 1960 by L-Aspartate for Enhanced Itaconic Acid Production. Applied Biochemistry and Biotechnology, 177(3):595-609.